PB84-168368

Acidification of Rain by the Oxidation of Dissolved SO2 and the Absorption of HNO3

(U.S.) Environmental Sciences Research Lab.
Research Triangle Park, NC

1984

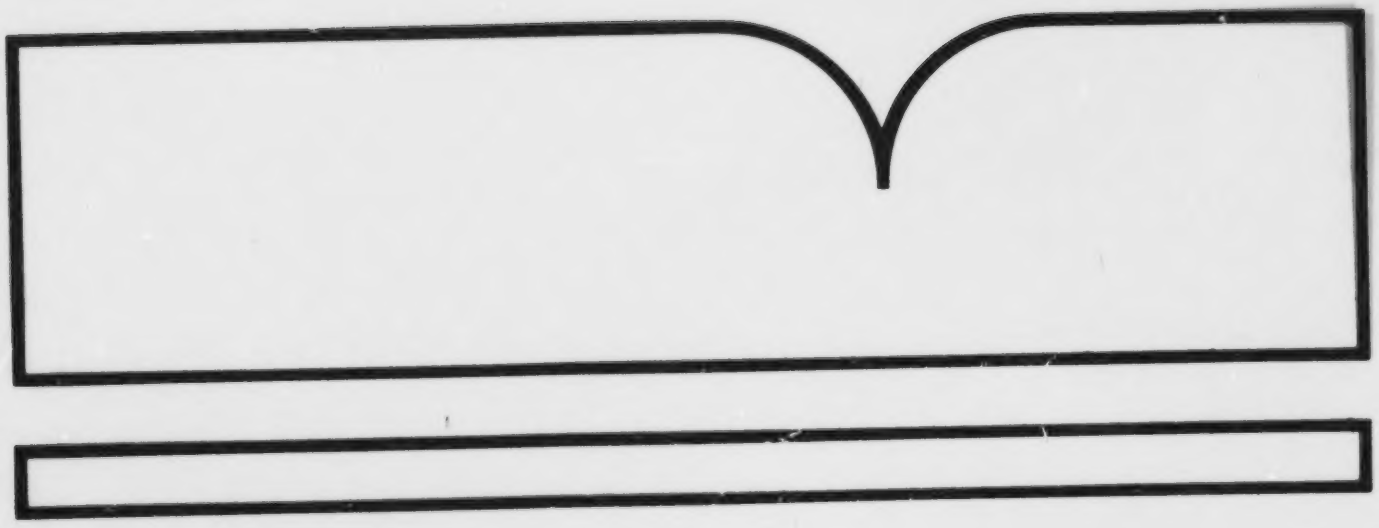

U.S. Department of Commerce
National Technical Information Service
NTIS

PB84-168368

EPA-600/D-84-081
1984

ACIDIFICATION OF RAIN BY THE OXIDATION OF DISSOLVED SO_2 AND THE ABSORPTION OF HNO_3

J.L. Durham and H.M. Barnes
Environmental Sciences Research Laboratory
U.S. Environmental Protection Agency
Research Triangle Park, NC 27711

and

J.H. Overton, Jr.
Environmental Sciences
Northrop Services Inc.
Research Triangle Park, NC 27709

ENVIRONMENTAL SCIENCES RESEARCH LABORATORY
OFFICE OF RESEARCH AND DEVELOPMENT
U.S. ENVIRONMENTAL PROTECTION AGENCY
RESEARCH TRIANGLE PARK, NC 27711

REPRODUCED BY
NATIONAL TECHNICAL
INFORMATION SERVICE
U.S. DEPARTMENT OF COMMERCE
SPRINGFIELD, VA. 22161

TECHNICAL REPORT DATA *(Please read Instructions on the reverse before completing)*		
1. REPORT NO. EPA-600/D-84-081	2.	3. RECIPIENT'S ACCESSION NO. PB84 168368
4. TITLE AND SUBTITLE ACIDIFICATION OF RAIN BY THE OXIDATION OF DISSOLVED SO_2 AND THE ABSORPTION OF HNO_3		5. REPORT DATE 1984
		6. PERFORMING ORGANIZATION CODE
7. AUTHOR(S) Jack L. Durham, H. M. Barnes, and John H. Overton*		8. PERFORMING ORGANIZATION REPORT NO.
9. PERFORMING ORGANIZATION NAME AND ADDRESS Same as Box 12		10. PROGRAM ELEMENT NO. ACVN1A/01 Task 2347 FY-84
		11. CONTRACT/GRANT NO.
12. SPONSORING AGENCY NAME AND ADDRESS Environmental Sciences Research Laboratory - RTP, NC Office of Research and Development U.S. Environmental Protection Agency Research Triangle Park, North Carolina 27711		13. TYPE OF REPORT AND PERIOD COVERED
		14. SPONSORING AGENCY CODE EPA/600/09

15. SUPPLEMENTARY NOTES

*Northrop Services, Inc., Research Triangle Park, North Carolina 27709

16. ABSTRACT

Most calculations have been performed for sub-cloud acidification of rain. The roles of chemical oxidation kinetics, mass transport rates for gas scavenging, and the raindrop size distribution have been examined. H_2O_2 (10 ppb) greatly dominates O_3 and Mn^{2+} in oxidizing dissolved SO_2 to form H^+ and SO_4^{2-}. HNO_3 is important for acidification of rain and it also slightly inhibits SO_4^{2-} formation. Sub-cloud scavenging of H_2O_2 and HNO_3 is mass transport limited, thus causing the acidification of rain to be mass-transported limited. The Marshall-Palmer distribution results in greater predictions of acidity, (SO_4^{2-}), and (NO_3^-) than the best distribution for raindrops larger than 0.2 mm. Sub-cloud acidification of rain is strongly dependent on: (a) the concentrations of SO_2, H_2O_2, and HNO_3, (b) the sub-cloud fall distance, and (c) the raindrop size distribution.

17. KEY WORDS AND DOCUMENT ANALYSIS		
a. DESCRIPTORS	b. IDENTIFIERS/OPEN ENDED TERMS	c. COSATI Field/Group
18. DISTRIBUTION STATEMENT RELEASE TO PUBLIC	19. SECURITY CLASS *(This Report)* UNCLASSIFIED	21. NO. OF PAGES 73
	20. SECURITY CLASS *(This page)* UNCLASSIFIED	22. PRICE

EPA Form 2220-1 (9-73)

NOTICE

This document has been reviewed in accordance with U.S. Environmental Protection Agency policy and approved for publication. Mention of trade names or commercial products does not constitute endorsement or recommendation for use.

INTRODUCTION

An awareness of the acidification of eco-systems and the possible adverse effects were recognized in Europe over a decade ago.[1,2] In The United States, there does not yet exist sufficient observations from a continuous monitoring network to establish clearly a trend in rain water acidification. However, the importance of the problem has been recognized[3], and research and development to define the acid deposition patterns and eluidate causal relationships are underway.[4] Among the important questions regarding the acidification of rain droplets is the significance of the coupling of non-linear mass transport and chemical processes. It should be expected that the rate and degree of acidification of rain may be influenced by: (a) the concentrations of oxidizing agents (e.g., H_2O_2, O_3, and catalytic metal and non-metal ions), mineral acid precursors (e.g., SO_2 and NO_2), and acidic gases, (b) the chemical oxidation rates expressions, and (c) the rate of absorption of the gaseous reactants by the rain droplets. In this chapter, a sub-cloud scavenging/chemical reaction event model is presented to investigate these interacting non-linear processes.

The model includes material balances on the microscopic scale only. Since it does not include macroscale material balances, energy balances, and momentum balances, it is not directly applicable to the description of environmental events, especially convective storms. However, the model does provide insight on the role of acidification chemistry and is expected to be a guide in the development of the cloud chemistry module of the Eulerian Regional Acid Deposition Model (RADM), which is under development as a part of the National Acid Precipitation Assessment Program.[4] The RADM will be a predictive model that will account for macroscale material, energy, and momentum balances.

THE PHYSICAL AND CHEMICAL MODEL

Rain System Model

The atmosphere is divided into two regions (see Fig. 1) with respect to the vertical, each with the constant temperature, 25:C. Raindrops are formed in the upper region of the rain cloud. They are in equilibrium with CO_2 and may contain Mn, SO_4^{2-} and other chemical species that a drop could reasonably be expected to have prior to leaving the cloud.

The lower or polluted region extends from the cloud base to the ground and may contain the trace gases SO_2, O_3, H_2O_2, CO_2, NH_3 and HNO_3. Raindrops fall from the upper region through the lower region. They absorb the trace gases and decrease their ambient concentrations. In the liquid drop the absorbed gases react, alter the pH, produce NO_3^-, SO_4^{2-} and other products.

Raindrops, in our model, are rigid spheres of water; they do not grow, evaporate, collide, or scavenge each other; i.e. each drop that enters the polluted region maintains its size, shape and temperature (25°C) throughout its fall.

Mathematical Model

The relevant equation to solve is the equation of continuity with chemical reactions,

$$\partial C/\partial t + \nabla\cdot\underline{v}C = D\nabla^2 C + \Gamma(C) \qquad (1)$$

where $\underline{v}$ = velocity of medium, D = diffusion coefficient, C = concentration, and Γ = chemical reaction rate (a function of concentration). In principle this equation should be solved inside and outside of the drop; however, this is beyond the scope of this work. Instead we consider the interior of the drop and average Eq. (1) over the drop volume. Performing this and using Green's theorem one obtains

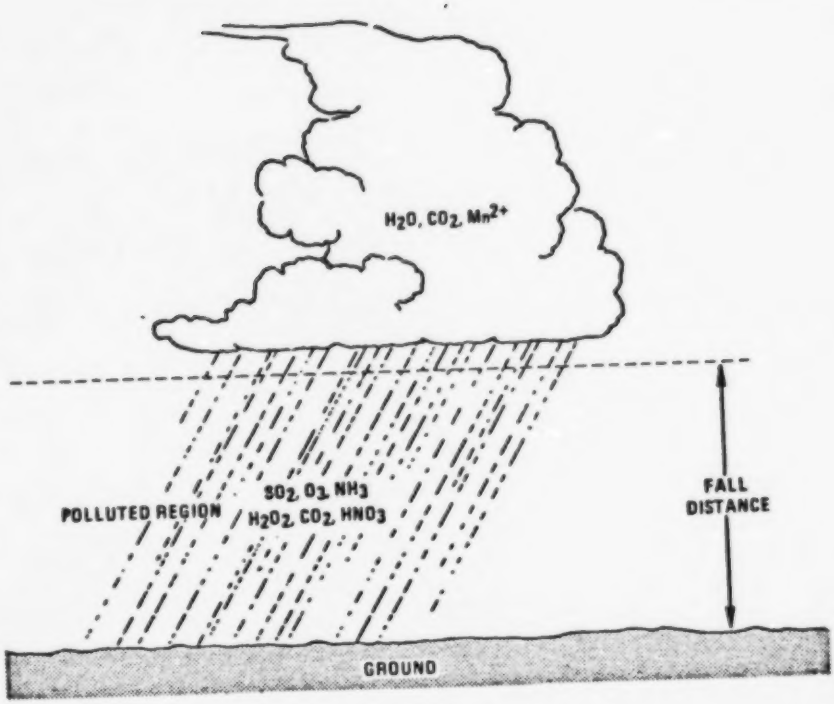
H_2O, CO_2, Mn^{2+}
SO_2, O_3, NH_3
H_2O_2, CO_2, HNO_3
POLLUTED REGION
FALL DISTANCE
GROUND

1

$$d\bar{C}/dt = -(1/V)\oint\!\!\!\oint_A \hat{r}\cdot\underline{v}C\,dA + (1/V)\oint\!\!\!\oint_A D\hat{r}\cdot\bar{v}C\,dA + \bar{\Gamma} \qquad (2)$$

where the over bar indicates volume average, dA = surface element, $\hat{r}$ = unit radius vector, $\oint\!\!\!\oint$ = surface (of drop) integral and $V = (4/3)\pi R^3$.

On the surface of the drop $\hat{r}$ is perpendicular to $\underline{v}$, thus the first term on the right hand side of Eq. (2) is zero. The second term represents the net transfer of component C on the liquid phase side of gas-liquid interface at the interface ($-D\hat{r}\cdot\nabla C$ is the point wise current perpendicular to the surface).

Based on the work of Baboolal et al.[5] and Frossling[6] and on concept of a gas

$$\oint\!\!\!\oint D\hat{r}\cdot\bar{v}C\,dA = 4\pi R^2 k_g(C_g - H\bar{C}_A), \qquad (3)$$

where C_g = the bulk gas phase concentration, $\bar{C}_A$ = the average liquid interfacial value, k_g = gas phase mass transfer coefficient, and H = Henry's law constant (see Table I).

Thus, we can write, setting $t = z/u$,

$$d\bar{C}/dz = (30k_g/uR)(C_g - H\bar{C}_A) + \bar{\Gamma}/u \qquad (4)$$

where z = vertical distance of drop fall and u = the (constant) fall velocity.

The fall velocity u is taken from an equation of Markowitz[7] that was "derived from Best[8]":

$$u = 9.58\{1 - \exp[-(R/0.885)^{1.147}]\} \qquad (5)$$

TABLE I. GAS PHASE DIFFUSION COEFFICIENTS AND HENRY'S LAW CONSTANTS

Species	D^*, cm^2/sec	H	Source of H values
CO_2	0.166	1.2	Perry & Chilton[9]
O_3	0.157	3.36	Perry & Chilton[9]
SO_2	0.136**	0.0332	Hales & Sutter[10]
HNO_3	0.136	0.46E-6	Abel & Neusser[11]; McKay[12]
H_2O_2	0.186	0.557E-6	Martin & Damschen[13]
NH_3	0.234	6.7E-4	Perry & Chilton[9]

*D_s = [(molecular weight of SO_2)/(molecular weight of species s)]$^{0.5} D_{SO_2}$

**Fish & Durham[14]

This formula represents terminal velocities very well over the range of drop sizes of interest.[15]

For the mass transfer coefficient, k_g, we use the Frossling[6] correlation:

$$Sh = \alpha + \beta(2\rho Ru/\nu)^{1/2}(\nu/D)^{1/3}, \tag{6}$$

where Sh = Sherwood number = $2Rk_g/D$

ν = kinematic viscosity

$\alpha = 2.0$

$\beta = 0.6$

The values used for the diffusion coefficents, D, are given in Table I.

According to Beard and Pruppacher[16] the dependence of Sh on the constants α and β varies from investigator to investigator; however, the exponents 1/2 and 1/3 are agreed upon over the range of drop sizes of interest. They also give $\alpha = 1.56$ and $\beta = 0.616$; these values are not significantly different from the values we use and give some idea as to the possible error in a calculation of k_g.

Equation (4) cannot be solved unless $\bar{C}_A$ and $\bar{\Gamma}$ are specified, which of course requires a complete solution. To avoid that and to simplify the problem, we define

$$\bar{C}_A \equiv \bar{C} \tag{7a}$$

and

$$\bar{\Gamma} \equiv \Gamma(\bar{C}). \tag{7b}$$

Thus, generalizing the above to more than one species, we solve a set of non-linear coupled differential equations of the form

$$d\bar{C}_s/dz = (30k_{gs}/uR)(C_{gs} - H_s\bar{C}_s) + \Gamma_s(\underline{\bar{C}})/u, \quad s = 1(1)N \tag{8}$$

where $\bar{C}_s$ = the average aqueous phase concentration of species s,

$\underline{\bar{C}}$ = the vector of average concentrations, $\{C_s\}_{s=1}^{N}$

N = the number of chemical species.

The assumptions and simplifications that lead to Eq. (8) are subject to criticism, especially Eq. (7). These definitions are equivalent to the assumption that the material in a drop is nearly uniformally spread throughout the drop. This will be the case as the drop approaches saturation; however, this in general is not the situation. If the drop were throughly mixed then constant concentrations could be expected. In this case a two film model, such as developed by Carmichael and Peters,[17] may be appropriate. If the mass transfer were gas phase limited then this model and ours would be equivalent. In any case the concept of a throughly mixed or constant concentration internal core is not indicated by Baboolal et al.[5] who solved Eq. (1) inside and outside drops for SO_2 scavenging. We are not able to determine at this time how good the present drop model formulation is but we have no reason to doubt that qualitative conclusions would remain the same given a more sophisticated model.

In order to simulate the chemistry in a rain event after a given fall distance consideration must be given to all size drops. To do this we have considered the raindrop size distributions in air developed by Best[8] and by Marshall and Palmer.[18]

Best density function:

$$f_B(R) = N_B R^{1.25} \exp[-(2R/a)^{2.25}], \tag{9}$$

where

$a = 1.3p^{0.232}$,

p = precipitation rate, mm/hr.

N_B = normalization constant

Marshall-Palmer density function:

$$f_{MB}(R) = N_{MP}R^3\exp[-2RE], \tag{10}$$

where

$E = 4.1p^{-0.21}$

N_{MP} = constant independent of p.

Figure 2 presents plots of f_B and f_{MP} versus raindrop radius for two precipitation rates. The curves begin at R = 0.1 mm, which we have arbitrarily taken to be the minimum drop size. A discussion of the effect of different size distributions and different minimum radii has been presented by Levine and Schwartz[19]; in any case, we have chosen to work with the Best distribution.

The average ground level concentration, $\bar{\rho}_s$, of a chemical species s is computed in two steps. First, the following average (at fall distance x) is computed:

$$\bar{\rho}_s = F^{-1}\int_{0.1}^{2.5} u(R)\bar{C}_s(z,R)f(R)dR \tag{11}$$

where

$$F = \int_{0.1}^{2.5} u(R)f(R)dR$$

This average does not take into account the continuing chemical reactions in in the bulk fluid in the collector. Thus, using $\bar{\rho}_s$, s = 1(1)N, as initial values, the chemical reactions are allowed to continue (with no mass transport) for a time at least long enough to establish chemical equilibrium for the reversible reactions.

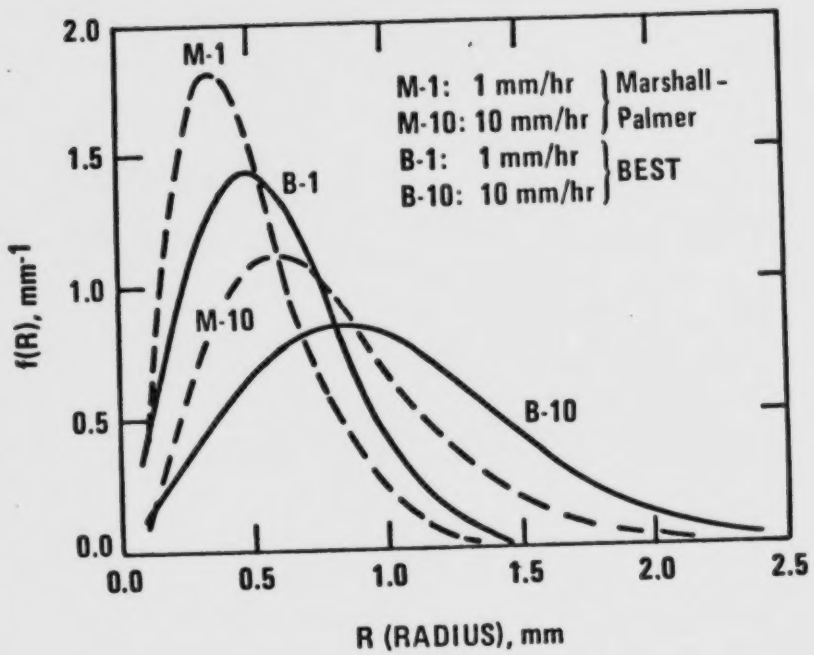
2.0
1.5
1.0
0.5
0.0
f(R), mm⁻¹
M-1
B-1
M-10
B-10
M-1: 1 mm/hr
M-10: 10 mm/hr
Marshall - Palmer
B-1: 1 mm/hr
B-10: 10 mm/hr
BEST
0.0
0.5
1.0
1.5
2.0
2.5
R (RADIUS), mm

2

Time dependence of gaseous and liquid chemical species is obtained in steps. The vertical gaseous concentrations are independent of height (no gas phase concentration gradients) and are held constant while the set of equations, Eq. (8), are integrated from the cloud base to the ground for several values of R. A raindrop size distribution, Eqs. (9) or (10), is used with these solutions to estimate Eq. (11) numerically. The reactions are then allowed to continue in order to establish the ground level rain water concentrations. After this set of calculations the ambient gaseous values, held constant during the above calculations, are modified to take into account the material lost or gained by the falling rain for the time of the step (five minutes - the reasons for which are discussed later). This step process can be repeated with the net result, as time (number of step) increases, of time varying gas and liquid phase concentrations.

The above assumes that the raindrop distribution is independent of fall distance and time. This assumption is partly justified by the fact that 92% (rain time = 10 mm/hr Best distribution) of the initial model drops will have fallen 1000 meters in the first 3.7 minutes of the rain event, and 97% will have fallen the 1000 meters in 6.5 minutes after the first drops hit the ground. Thus the raindrop distribution for a 10 mm/hr rain rate is essentially developed at 1000 meters after the first four minutes of the beginning of the rain event at the ground. Therefore we interpret our results as obtained from rain samples collected after the first few minutes, at least, of the beginning of the rain event. This interpretation will be reasonable if the ambient or liquid concentrations at a given height do not change very much during the time of interest. For example, in the simulation of a 1000 meter, 10 mm/hr (Best) rain event (initially, $[H_2O_{2(g)}] = [SO_{2(g)}] = 5$ ppb, $[O_{3(g)}] = 50$ ppb, $[NH_{3(g)}] = [HNO_{3(g)}] = 2$ ppb) ambient $[H_2O_{2(g)}]$ was reduced by ~ 9% each 5 minutes while other significant species decreased by less than this amount.

Chemical Reaction Model

In Table II, the chemical reactions selected for determining the acidification of falling raindrops are listed. Equations 1-8 are the reversible reactions for the CO_2-SO_2-HNO_3-NH_3-H_2O system. Equations 9-11 are for sulfate production by ozone oxidation. Experimental reaction rates have been reported by Penkett[29] and Erickson et al.[23] for the S(IV)-O_3 aqueous system. Penkett reported an overall rate rather than in terms of the contributions of ozonation of SO_2, HSO_3^-, and SO_3^{2-}. Erickson et al. reported the fractional contribution of the individual S(IV) species. Equation 12 is the irreversible S(IV) oxidation by H_2O_2. The reaction rate constant given in Table II is a compromise among those values reported by Martin and Damschen[13], Penkett et al.[26,24] and Hoffman and Edwards[25]. Equation 13 is the manganese catalyzed S(IV) oxidation reaction. The reaction rate expression was obtained from Penkett et al.[27] after conversion to units of mole, liter, second. Equation 14 represents the carbon catalyzed S(IV) oxidation that has been studied by Brodzinsky et al.[28] Although this reaction may be of some importance in urban aerosol growth, our calculations show it is unimportant for acidification of rain in our model. Using a rain water concentration of 240 μg/ℓ carbon and a rain event time of 5 minutes results in sulfate formation less than 1 μM. Therefore, we have not used Eq. 14 in any of our simulations.

TABLE II. KINETIC MECHANISM

Reaction	Rate[a]		Source	Reference
1. H_2O	$\overset{1.3E-3}{\underset{1.3E+11}{\rightleftharpoons}}$	$H^+ + OH^-$	Eigen et al.	20
2. $CO_2 + H_2O$	$\overset{2.4E-2}{\underset{4.9E+4}{\rightleftharpoons}}$	$HCO_3^- + H^+$	Himmelblau & Babb (by extrapolation to 25°C)	21
3. HCO_3^-	$\overset{1.0E-4}{\underset{1.4E+4}{\rightleftharpoons}}$	$CO_2 + OH^-$	Eigen et al.	20
4. $SO_2 + H_2O$	$\overset{3.4E+6}{\underset{2.0E+8}{\rightleftharpoons}}$	$H^+ + HSO_3^-$	Eigen et al.	20
5. HSO_3^-	$\overset{1.0E+4}{\underset{1.0E+11}{\rightleftharpoons}}$	$SO_3^{2-} + H^+$	Erickson & Yates Erickson et al.	22 23
6. HNO_3	$\overset{2.2E+9}{\underset{1.0E+8}{\rightleftharpoons}}$	$H^+ + NO_3^-$	McKay	12
7. NH_4^+	$\overset{2.5E+1}{\underset{4.3E+10}{\rightleftharpoons}}$	$NH_3 + H^+$	Eigen et al.	20
8. NH_3	$\overset{6.0E+5}{\underset{3.4E+10}{\rightleftharpoons}}$	$NH_4^+ + OH^-$	Eigen et al.	20
9. $O_3 + SO_2$	$\xrightarrow{5.9E+2}$	$2H^+ + SO_4^{2-}$	Erickson et al.	23
10. $O_3 + SO_3^{2-}$	$\xrightarrow{2.2E+9}$	SO_4^{2-}	Erickson et al.	23
11. $O_3 + HSO_3^-$	$\xrightarrow{3.1E+5}$	$H^+ + SO_4^{2-}$	Erickson et al.	23
12. $H_2O_2 + SO_2$	$\xrightarrow{1.24E+6}$	$2H^+ + SO_4^{2-}$	Hoffman & Edwards Penkett et al. Martin & Damschen	25 26 13
13. SO_2 (+ Mn^{2+})	$\xrightarrow{\text{(see "b \& c")}}$	$2H^+ + SO_4^{2-}$	Penkett et al.	27

(CONTINUED)

TABLE II. (Continued)

Reaction	Rate	Source	Reference
14. SO_2 (+ C(0))	$\xrightarrow{\text{(see "c")}}$ $2H^+ + SO_4^{2-}$	Brodzinsky et al.	27

a. units: mole, liter, second

b. $d[H^+]/dt = d[SO_4^{2-}]/dt$

$= (1.4E+5)[HSO_3^-]^{1.5}[Mn^{2+}]$

$[S(IV)] = [HSO_3^-]$

c. we have assumed that the reaction produces 2 H^+.

Various other potential catalysts and oxidants were considered in this investgation and eventually rejected as being unimportant. These included Fe(III), V(IV), and various N-species.

Fe(III) has been considered by Overton et al.[30]; they used the rate constant data of Brimblecombe and Spedding[31] for the Fe(III) catalyzed oxidation of S(IV). In the S(IV)-O_3-Fe(III) system, the contribution of Fe(III) catalysis to SO_4^{2-} formation is less than 10% of the total. Since more efficient oxidants (Mn(II) and H_2O_2) are included in the current simulations, the Fe(III) contribution would be even smaller. Thus, it has been neglected.[27]

Simularly, considerations of the NO_2 aqueous phase reactions leading to HNO_3 have resulted in their being neglected here. The Henry's law constant for NO_2 is ~ 1, which is sufficiently low to eliminate bulk aqueous reactions leading to the formation of H^+, NO_3^-, or SO_4^{2-}. However, N_2O_4 is soluble, and it can be formed as follows:

$$2NO_2 \underset{7.7E+3}{\overset{5.0E+8}{\rightleftharpoons}} N_2O_4.$$

Dinitrogen tetroxide can undergo further reaction with water:

$$N_2O_4 + H_2O \underset{}{\overset{2.0E+2}{\rightleftharpoons}} HNO_3 + HNO_2$$

Previous calculations[32] have demonstrated that 10 ppb of NO_2 produced insignificantly low quantities ($< 1nM$) of NO_2^- and NO_3^- in the aqueous phase. It is warranted to ignore these reactions for our sub-cloud scavenging simulations. However, there is preliminary evidence[33] that NO_2 may be oxidized rapidly by H_2O_2 in aqueous systems.

Martin et al.[34] investigated S(IV) oxidation by various metal catalysts including Fe(III), Mn(II), Pb(II), VO(II), Cu(II), and Co(II). They concluded that only Fe(III) and Mn(II) caused measurable oxidation in the SO_2-O_2 aqueous system. We have already discussed the reasons for neglecting the Fe(III) catalytic oxidation. Based on the results of Martin et al.[34] and Penkett et al.[27], we neglect metal catalysis, except for that by Mn(II).

Simulation Parameters

In Table III we list the basic parameters used in our simulations. We have attempted to use reported or realistic estimates of values for the gas phase concentration ranges. For example, $H_2O_2(g)$ has been reported at concentrations exceeding 30 ppb in northeastern U.S.[35] H_2O_2 measurement methodology is not yet firmly established, so we regard our selection of the range of 2 to 10 ppb as reasonable. $HNO_3(g)$, formed principally by the reaction of NO_2 and HO radicals often obtains concentrations as high as 10 ppb in the northeastern U.S.[36] The Mn(II) concentration selected for these simulations was based on a range of values reported by Penkett et al.[27] for 9 rain water samples. They reported Mn(II) levels of 0.1 μM to 1 μM. In our calculations, we have used 10 μM so that any effect on sulfate or pH due to Mn(II) catalysis might be considered an upper limit.

TABLE III. BASIC PARAMETERS USED IN SIMULATIONS

Gases		Aqueous Solution		Other
Species	Concentration	Species	Concentration	
$[SO_2]$	= 0 - 20 ppb	$[H^+]$	= 3.3 μM; pH = 6.3	Raindrop radii: 0.1 - 2.5 mm
$[O_3]$	= 0 - 50 ppb	$[OH^-]$	= 4.3 nM	Fall distances: 1000 m, 3000 m
$[H_2O_2]$	= 0 - 10 ppb	$[CO_2]$	= 11 μM	
$[NH_3]$	= 0 - 10 ppb	$[HCO_3^-]$	= 2.33 μM	
$[CO_2]$	= 320 ppm	[Mn(II)]	= 0 - 10 μM	
$[HNO_3]$	= 0 - 10 ppb			

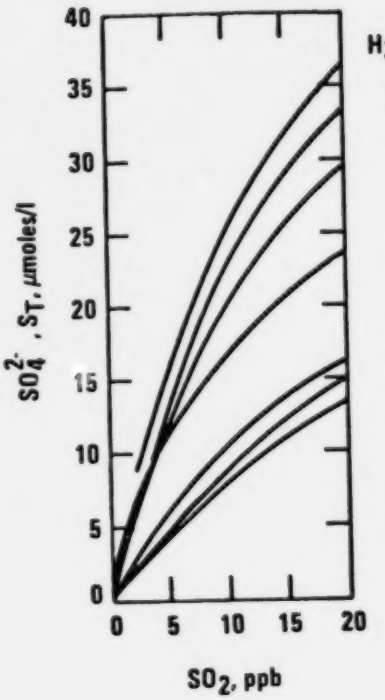

H_2O_2	O_3	Mn^{2+}	NH_3
5	50	5	5
5	50	5	0
5	0	0	0
0	0	0	5
0	50	0	0
0	0	5	0
0	0	0	0

$[HNO_3]_g = 5$
Z = 1000 m
10 mm/hr, BEST

3

RESULTS AND DISCUSSION

Most of the data presented in this paper can be considered as corresponding to that of a 5 minute collection of rain water. The exception to this is several four hour rain event simulations. In addition the data can correspond to samples which are "immediately" analysed (5 minutes of continued reactions in the collector) or to samples in which the S(IV) is totally oxidized to sulfate -- referred to as 100% conversion. The latter procedure attempts to simulate the results of an analysis carried out a long time after sample collection (e.g., followed by oxidation due to a catalyst).

Relative Effectiveness of H_2O_2, Mn^{2+}, O_3, and NH_3 for SO_4^{2-} Formation in the Presence of $HNO_3(g)$ (100% Conversion).

In Figure 3 we demonstrate graphically the effect of specific oxidizing systems on sulfate production. Several important points should be noted here.

(1) H_2O_2 is the most significant oxidant of the three considered (H_2O_2, O_3, Mn^{2+}/O_2 catalysis). O_3 and Mn^{2+} do not differ dramatically from the uncatalyzed system (lowest curve). For example when $[SO_{2(g)}]$ = 20 ppb, the uncatalyzed SO_2/O_2 reaction results in about 12 $\mu\underline{M}$ SO_4^{2-}, the Mn^{2+}/O_2 system gives about 14 $\mu\underline{M}$ SO_4^{2-} and O_3 results in 16 $\mu\underline{M}$ SO_4^{2-}.

(2) Second to H_2O_2 is the effect of NH_3 on the system. This is not an effect

of oxidation, but rather reflects the increased solubility of SO_2 as NH_3 increases the pH. The effect is rather dramatic compared to O_3 or Mn^{2+}.

(3) Note the non-additivity and non-linearity of effects by the oxidants. For example, for $[H_2O_2]$ = 5 ppb, in reducing $[SO_{2(g)}]$ from 20 ppb to 10 ppb, sulfate in the rain water decreases only from about 29 μM to about 20 μM. Also the non-additivity of effects can be demonstrated by considering the case of $[SO_{2(g)}]$ = 20 ppb for each individual oxidant and then for all four together. For each individual oxidant system we have:

SO_2/O_2:	$[SO_4^{2-}]$ = 12 μM
$SO_2/O_2/Mn^{2+}$:	$[SO_4^{2-}]$ = 14 μM
SO_2/O_3:	$[SO_4^{2-}]$ = 16 μM
$SO_2/NH_3/O_2$:	$[SO_4^{2-}]$ = 23 μM
SO_2/H_2O_2:	$[SO_4^{2-}]$ = 29 μM

The total is 94 μM SO_4^{2-} if the effects were additive However, by examining the top curve in the figure we see a sample containing all four oxidants produces only about 36 μM SO_4^{2-}. The H_2O_2 is so much more effective and rapid in this system that the other oxidants are not contributing significantly. As previously stated in the model description this is a 5 minute rain event, and in that short period the SO_2/H_2O_2 kinetics control the final results.

Relative Effectiveness of H_2O_2 and O_3 on Acidification and SO_4^{2-} Formation (100% Conversion)

For a 5 minute rain event we have calculated pH and $[SO_4^{2-}]$ for raindrops with initial conditions of the simulation are $[SO_{2(g)}]$ = 10 ppb and $[HNO_{3(g)}]$ = 0. $[H_2O_{2(g)}]$ and $[O_{3(g)}]$ are the variables in Figure 4 for isolines of pH and $[SO_4^{2-}]$. The small negative slopes of the isolines indicate that H_2O_2 is more effective than O_3 by a factor of ~ 12 ppb/ppb for lowering the pH and for forming SO_4^{2-} for the conditions of the simulation.

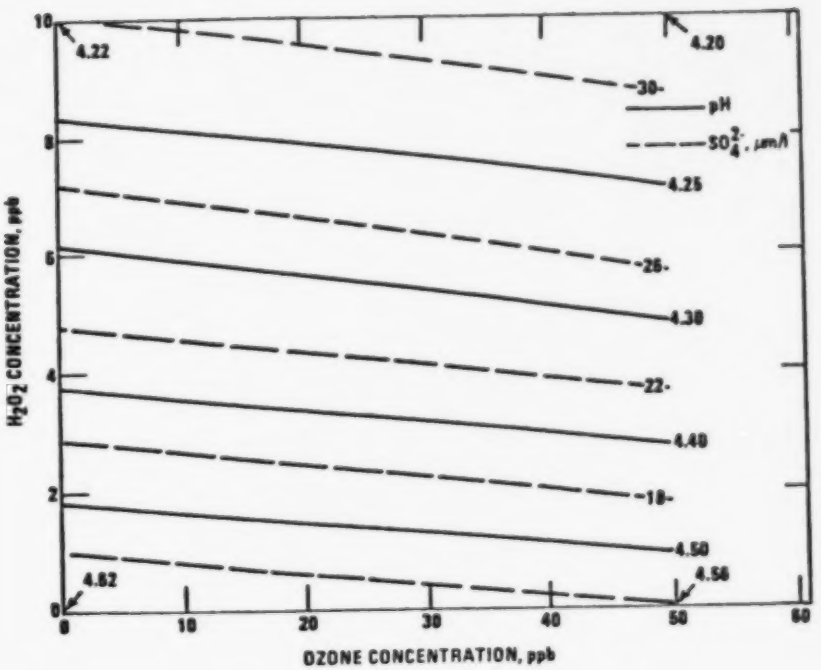
10
8
6
4
2
0
4.22
4.20
-30-
pH
SO_4^{2-}, μm/l
4.25
-26-
4.30
-22-
4.40
-18-
4.50
4.82
4.56
0
10
20
30
40
50
60
H_2O_2 CONCENTRATION, ppb
OZONE CONCENTRATION, ppb

4

Specifically, note the difference for $[H_2O_{2(g)}]$ = 10 ppb and $[O_{3(g)}]$ = 0 and 50 ppb; the pH declines from 4.22 to 4.20 for the two values of $[O_{3(g)}]$. When $[H_2O_{2(g)}]$ = 10 ppb the pH drops by 0.4 units from 4.62 (at $[H_2O_{2(g)}] = [O_{3(g)}]$ = 0 to 4.22), as compared to the previously stated 0.02 unit decrease in going from no ozone present to $[O_{3(g)}]$ = 50 ppb.

The presence of $HNO_{3(g)}$ (not shown on this figure) tends to enhance the relative effectiveness of H_2O_2 over O_3; that is due to the inhibition of the SO_2-O_3 reaction by H^+. There is no inhibition by H^+ in the SO_2-H_2O_2 aqueous system. Thus we conclude that in the presence or in the absence of HNO_3, H_2O_2 is a more effective oxidizer than O_3.

Relative Effectiveness of HNO_3 and H_2O_2 on Acidification and SO_4^{2-} Formation (100% Conversion).

Two specific cases are considered here to compare the relative effectiveness of H_2O_2 and HNO_3 (for a constant $[O_{3(g)}]$ = 50 ppb) in the presence of $[SO_{2(g)}]$ = 10 ppb and $[SO_{2(g)}]$ = 20 ppb (see Figures 5 and 6). This situation is analogous to the comparison for HNO_3 and SO_2 on acidification and sulfate formation which is discussed later in this section. In the present comparison (HNO_3 versus H_2O_2) the influence of Equation 12 in the kinetic mechanism is being evaluated. In Figure 5 $[H_2O_2] \leq [SO_{2(g)}]$ = 10 ppb and HNO_3 and H_2O_2 have approximately equal effectiveness for acidification; note however that sulfate formation is not strongly dependent on HNO_3. In Figure 6 for $[H_2O_2] < 10$ ppb and $[SO_{2(g)}]$ = 20 ppb the increase in the $[SO_{2(g)}]/[H_2O_2]$ results in the aqueous oxidation of S(IV) becoming more important and the acidification by HNO_3 less important. This conclusion is illustrated by the increase in slope of the pH isolines and their shift to lower values as the S(IV) concentration increases from 10 ppb to 20 ppb.

It should be noted here that these conclusions are based on our evaluation of the SO_2-H_2O_2 reaction rate constant; as discussed earlier, we have selected a compromise value among those reported in the literature.[13,25,26] If our value is later shown to be in error, these conclusions may require revision.

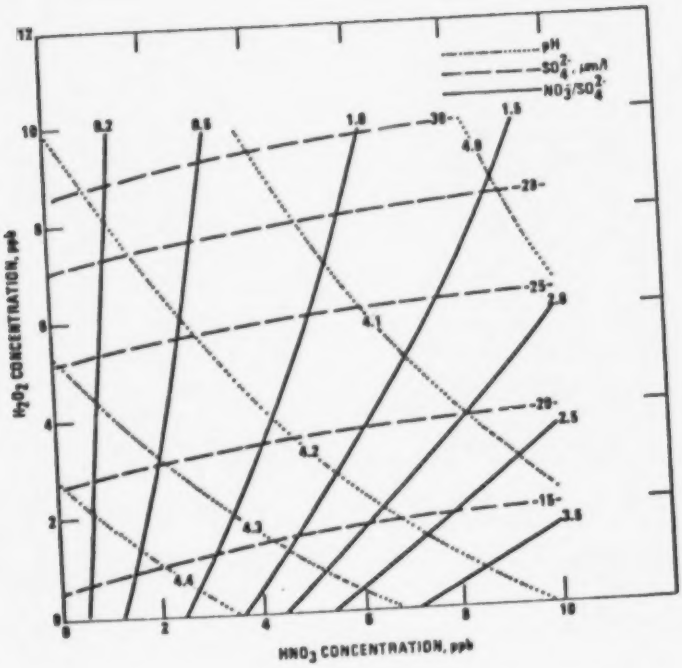
pH
SO_4^{2-}, μm/l
NO_3/SO_4^{2-}
H_2O_2 CONCENTRATION, ppb
HNO_3 CONCENTRATION, ppb
0
2
4
6
8
10
12
8.2
8.6
1.0
-30-
1.5
4.8
-28-
-25-
2.8
4.1
-20-
2.5
4.2
-15-
3.5
4.3
4.4

5

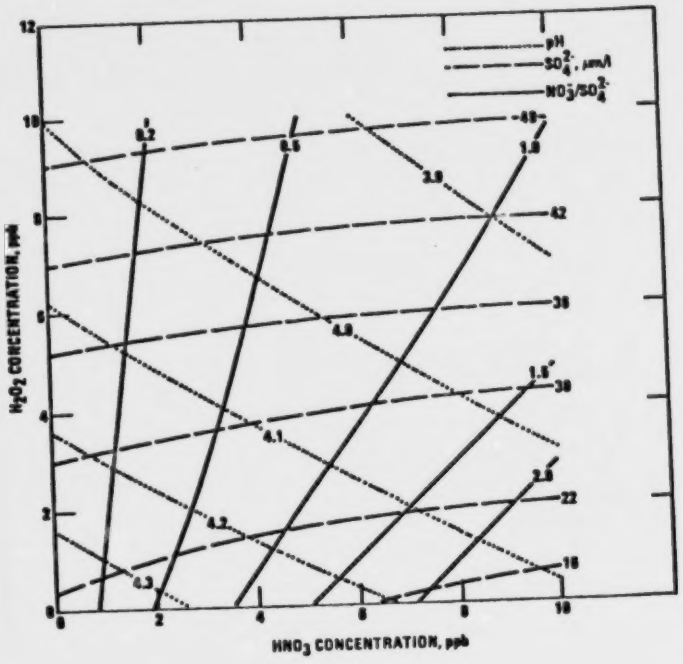
pH
SO_4^{2-}, μm/l
NO_3^-/SO_4^{2-}
H_2O_2 CONCENTRATION, ppb
HNO_3 CONCENTRATION, ppb
0.2
0.5
1.0
2.0
4.0
1.5
2.5
4.1
4.2
4.3
48
42
36
30
22
16
0
2
4
6
8
10
12

6

Relative Effectiveness of HNO_3 and SO_2 on Acidification and SO_4^{2-} Formation (100% Conversion).

Two rain events, one with $[H_2O_{2(g)}] = 0$ and the other with $[H_2O_{2(g)}] = 10$ ppb, are considered to compare the relative effectiveness of HNO_3 and SO_2 in the presence of $[O_{3(g)}] = 50$ ppb. The calculated isopleths for pH, $[SO_4^{2-}]$, and $[NO_3^-]/[SO_4^{2-}]$ for a 5 minute rain sample are shown in Figure 7 for $[H_2O_{2(g)}] = 0$. Note that this system has been considered elsewhere[32] with one important difference. In the reference article no further chemical reaction was allowed to occur after the rain event. In the current work all S(IV) is converted to sulfate after collection. The differences in results caused by this will be discussed elsewhere in this section.

In Figure 7, the negative slope of the pH isolines demonstrate the dominant role of HNO_3 in controlling the acidity of this system. It is also apparent from this figure that HNO_3 suppresses sulfate formation due to O_3 oxidation. For example, at $[SO_{2(g)}] = 15$ ppb, note that as the $[HNO_{3(g)}]$ increases from 0 to 10 ppb, $[SO_4^{2-}]$ decreases from 17.5 μM to less than 12.5 μM; at the same time acidity is increasing due to the inclusion of $HNO_{3(g)}$ in the rain droplets.

When $H_2O_{2(g)}$ at 10 ppb concentration is added to the system, the isolines change drastically. This effect is shown in Figure 8. The pH isolines becomes much steeper indicating more dependence on $[SO_{2(g)}]$ and are displaced to more acidic values, i.e. lower pHs. The $[SO_4^{2-}]$ isolines are essentially vertical indicating strong dependence on $[SO_{2(g)}]$ but almost no dependence on $[HNO_{3(g)}]$. For HNO_3 to contribute significantly to the acidity ($[NO_3^-]/[SO_4^{2-}] > 2$) the $[HNO_{3(g)}]$ must exceed $[SO_{2(g)}]$ by at least a factor of 1.3. For $[SO_{2(g)}] < [H_2O_{2(g)}] = 10$ ppb, the effectiveness of SO_2 is approximately 1.3 times that of HNO_3 for rain acidification; as $[SO_{2(g)}] > [H_2O_{2(g)}]$, the importance of $SO_{2(g)}$ in acidification declines. If $[SO_{2(g)}]$

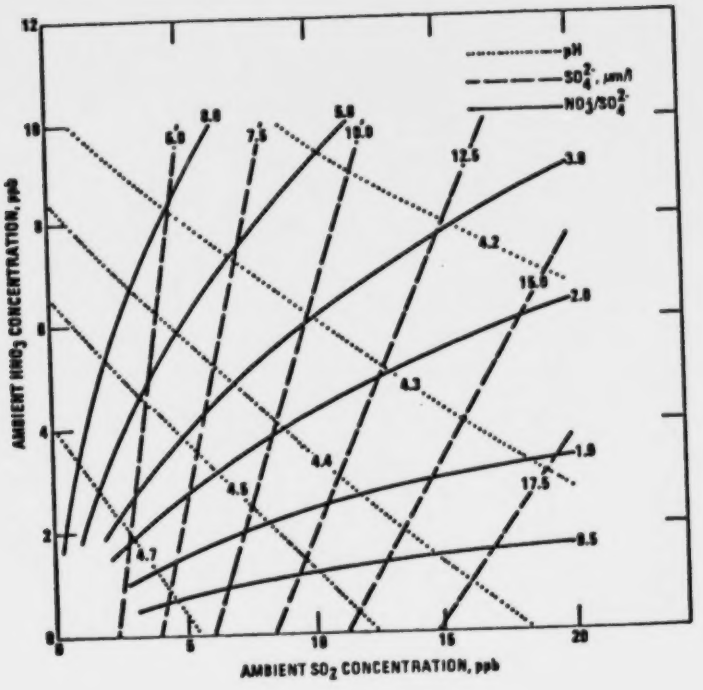
pH
SO_4^{2-}, μm/l
NO_3/SO_4^{2-}
AMBIENT HNO_3 CONCENTRATION, ppb
AMBIENT SO_2 CONCENTRATION, ppb
12
10
8
6
4
2
0
0
5
10
15
20
6.8
6.8
7.5
8.8
10.0
12.5
3.8
4.2
15.0
2.8
4.3
4.4
1.9
4.5
17.5
4.7
8.5

7

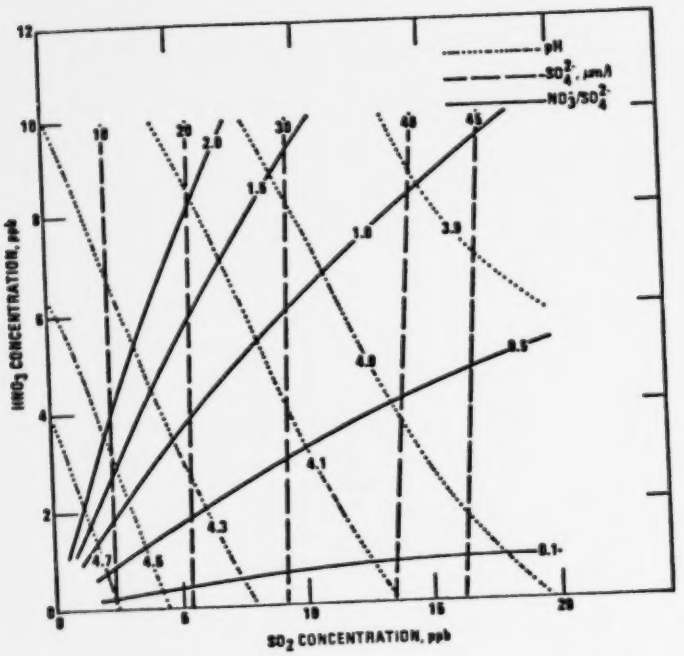
pH
SO_4^{2-}, μm/l
NO_3/SO_4^{2-}
HNO_3 CONCENTRATION, ppb
SO_2 CONCENTRATION, ppb
0
2
4
6
8
10
12
0
5
10
15
20
1.0
2.0
3.0
4.0
4.1
4.3
4.5
4.7
0.5
0.1

8

>7.5 ppb, then $[HNO_{3(g)}]$ must be greater than 10 ppb in order for $HNO_{3(g)}$ to dominate the acidification.

The behavior of the systems in these two figures demonstrate that in the presence of excess ozone ($[O_{3(g)}]$ = 50 ppb): (a) in the absence of $H_2O_{2(g)}$, $HNO_{3(g)}$ is more effective than SO_2 in acidifying rain and may limit SO_4^{2-} formation, but (b) in the presence of $H_2O_{2(g)}$ the roles are reversed; $SO_{2(g)}$ is more effective and SO_4^{2-} formation is only weakly dependent on $HNO_{3(g)}$. These conclusions are due to the relative effect of H_2O_2 on S(IV) oxidation and the pH dependence of the rate constant. In the absence of H_2O_2 as $[HNO_{3(g)}]$ increases, the pH in the droplet decreases. S(IV) solubility is decreased and its oxidation rate by O_3 decreases as pH decreases. Therefore acidification in this case in controlled by $HNO_{3(g)}$, which also tends to retard SO_4^{2-} formation. However, when H_2O_2 is introduced into the droplet the situation changes. The SO_2/H_2O_2 reaction rate increases with decreasing pH and it does so more dramatically than the reduced S(IV) solubility and S(IV)-O_3 reaction rate. Thus $[SO_{2(g)}]$ becomes more important and the SO_4^{2-} formation less dependent on HNO_3.

Effect of H_2O_2 and SO_2 on Acidification and Sulfate Formation (100% Conversion)

In Figures 9 through 12 we show that effect of HNO_3 on the resulting pH and SO_4^{2-} concentration for the SO_2-H_2O_2 system. These results are for a five minute rain event and 100% conversion of S(IV) to SO_4^{2-} after collection.

Let us first consider the effect on pH (see Figures 9 and 10) for $HNO_{3(g)}$ = 0 ppb and $HNO_{3(g)}$ = 5 ppb. For the situation in which $HNO_{3(g)}$ is absent pH decreases with increasing $SO_{2(g)}$ and increasing $H_2O_{2(g)}$. However, for $[SO_{2(g)}] < [HNO_{3(g)}]$, the pH is almost independent of $[H_2O_{2(g)}]$, as indicated by the nearly vertical isolines. There is effectively sufficient $H_2O_{2(g)}$ present even at the 1 ppb level to oxidize any absorbed $SO_{2(g)}$, whether its ambient concentration is 1 or 2 ppb. As the $[SO_{2(g)}]$ increases to 10 or 15 ppb, then the relative concentrations of

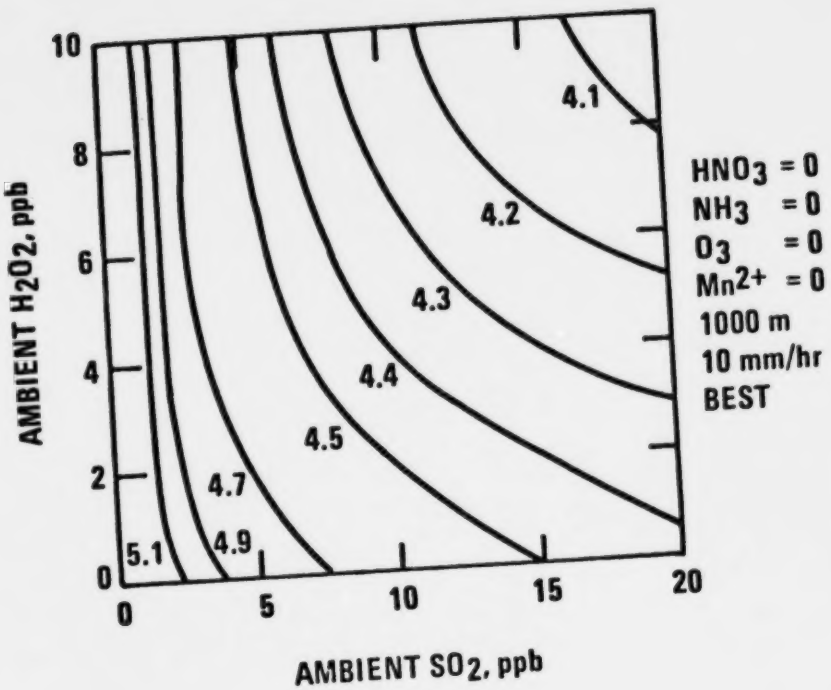
10
8
6
4
2
0
AMBIENT H_2O_2, ppb
0
5
10
15
20
AMBIENT SO_2, ppb
4.1
4.2
4.3
4.4
4.5
4.7
4.9
5.1
HNO_3 = 0
NH_3 = 0
O_3 = 0
Mn^{2+} = 0
1000 m
10 mm/hr
BEST

9

$SO_{2(g)}$ and $H_2O_{2(g)}$ become more significant and the pH isolines take on a non-linear shape.

In Figure 10 ($[HNO_{3(g)}] = 5$ ppb), we see the same general shape of the pH isolines for $[SO_{2(g)}] \leq 3$ ppb; that is, the pH is relatively independent of $[H_2O_{2(g)}]$ for very low $[SO_{2(g)}]$. As the $[SO_{2(g)}]$ and $[H_2O_{2(g)}]$ increase, the pH isolines become non-linear and the pH decreases. The effect of $[HNO_{3(g)}] > 0$ for $[SO_{2(g)}] >$ 5 ppb is to require less $H_2O_{2(g)}$ or $SO_{2(g)}$ to produce the same pH in the absence of $HNO_{3(g)}$. For example, when $[SO_{2(g)}] = 15$ ppb, $[H_2O_{2(g)}] = 0$, $[HNO_{3(g)}] = 0$, pH = 4.5. For $[HNO_{3(g)}] = 5$ ppb, $[SO_{2(g)}]$ need only be 5 ppb to result in the same pH value.

The other two figures (11 and 12) in this series reflect the influence of $HNO_{3(g)}$ on SO_4^{2-} formation. The shapes of the S_T isolines are similar to those for pH in the previous two figures. The two important observations here are: (1) except at high $[H_2O_{2(g)}]$, sulfate production is non-linear with regard to $[SO_{2(g)}]$; this is important when considering the implications of oxidant or SO_2 control to reduce sulfate levels and (2) the presence of $[HNO_{3(g)}]$ has the effect of requiring higher $[H_2O_{2(g)}]$ or $[SO_{2(g)}]$ to produce the same S_T as for $[HNO_{3(g)}] = 0$.

Effect of NH_3 and Oxidation

The analysis of a rain water sample, in many cases does not take place until hours, days or maybe many weeks after collection. During this time chemical reaction can continue and the properties of the solution may be in some respects very much different than initially. The two ways which we can report the simulation data represent the two extremes of no continued conversion of S(IV) to SO_4^{2-} and 100% conversion. These two extremes may lead to different results qualitatively as well as quantitatively. This is especially true when NH_3 is present and is illustrated in Figures 13 through 17.

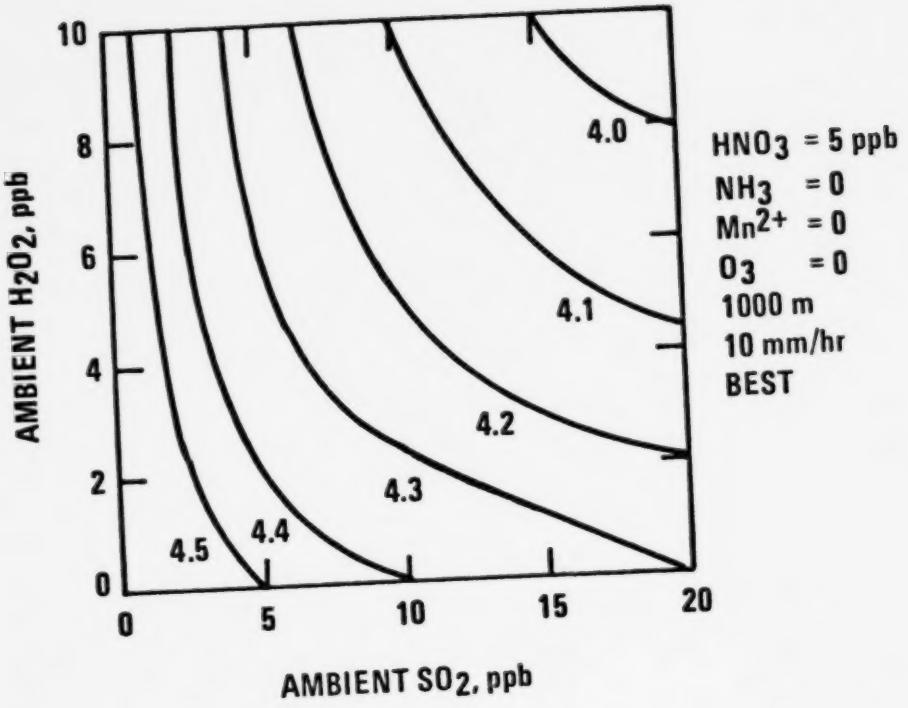
AMBIENT H_2O_2, ppb
10
8
6
4
2
0
0
5
10
15
20
AMBIENT SO_2, ppb
4.0
4.1
4.2
4.3
4.4
4.5
HNO_3 = 5 ppb
NH_3 = 0
Mn^{2+} = 0
O_3 = 0
1000 m
10 mm/hr
BEST

10

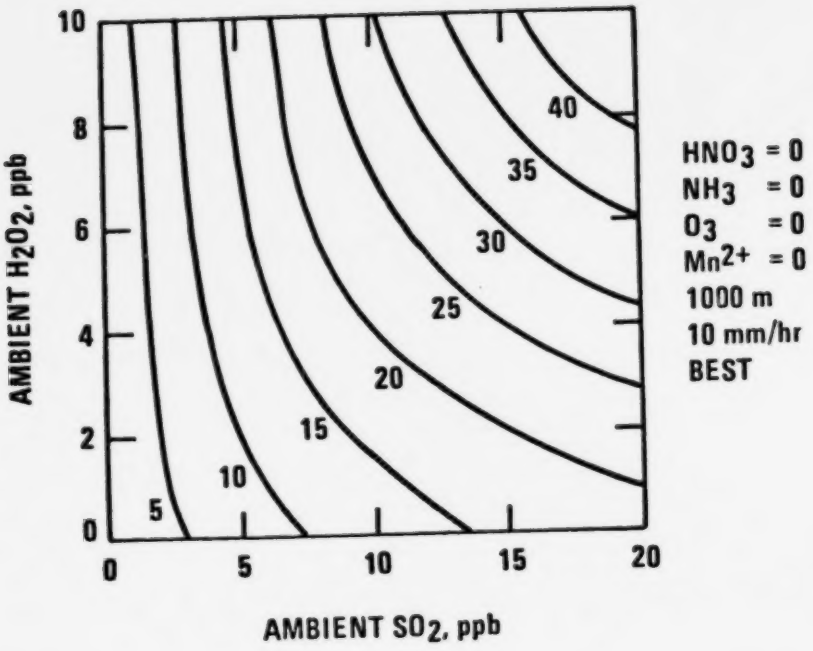
AMBIENT H_2O_2, ppb
AMBIENT SO_2, ppb
0
2
4
6
8
10
0
5
10
15
20
5
10
15
20
25
30
35
40
HNO_3 = 0
NH_3 = 0
O_3 = 0
Mn^{2+} = 0
1000 m
10 mm/hr
BEST

11

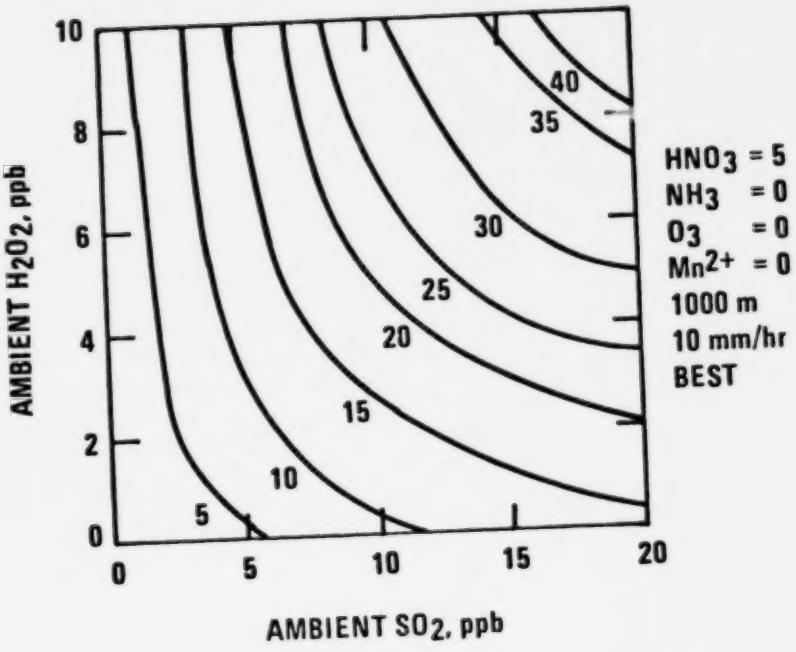
AMBIENT H_2O_2, ppb
AMBIENT SO_2, ppb
0
2
4
6
8
10
0
5
10
15
20
5
10
15
20
25
30
35
40
HNO_3 = 5
NH_3 = 0
O_3 = 0
Mn^{2+} = 0
1000 m
10 mm/hr
BEST

12

other hand for a given $[NH_3] > 0$, the S(IV) uptake decreases for increasing O_3. Thus, in the presence of a constant level of NH_3, an increasing $[O_3]$ will further acidify the droplets through the oxidation of HSO_3^- and cause the solubility of total S(IV) to decrease. The result is a reduction in S_T of the collected rain for increasing $[O_{3(g)}]$.

Figure 14 illustrates the effect of completion of oxidation of all S(IV) in the collector. In the case of no ambient O_3, it is seen that NH_3 greatly influences the pH of the rain entering the collector and not allowed to continue to react; however, if complete S(IV) oxidation occurs in the collector, there is not much influence on the final pH. An increase in ambient O_3 causes the differences in the unreacted and completely reacted S(IV) pH isolines to decrease. As noted above, as the O_3 oxidizes the S(IV) in the droplets, the solubility of S(IV) decreases, resulting in less S(IV) reaching the collector and available for oxidation.

This inhibiting aspect is not just a property of O_3; any oxidizer will do. In Figures 15 and 16 are presented the effect of H_2O_2, in the presence of NH_3, on the production of sulfate and acidity as a result of a 100% conversion after collection. These curves are more complex than those for O_3. Sulfate, for increasing $[H_2O_2]$ and $[NH_3] > 0$, decreases, then increases to a level as high or higher than for $[H_2O_2] = 0$. At the higher levels of NH_3 (8, 10 ppb), H_2O_2, just as O_3, has an insignificant effect on SO_2 uptake. The pH curves, Figure 16, also have some structure; for $NH_3 > 0$, pH increases and then decreases with increasing H_2O_2. Thus, H_2O_2 in the presence of NH_3 may inhibit the production of acidity as well as SO_2 absorption.

The inhibiting phenomenon can be explained in terms of both chemistry and mass transfer. Chemically, $SO_{2(aq)}$ is in equilibrium with the other S(IV) species, even during the oxidation. As the pH increases, due to the introduction of NH_3, the relative S(IV) concentration of $SO_{2(aq)}$ decreases. In our

simulations, the $[SO_{2(aq)}]$ may also decrease; that lowers the back pressure for mass transfer and increases the influx of SO_2 into the droplets. That is the reason for the increase in SO_2 uptake by NH_3. Now, an oxidizer lowers the pH, which tends to increase $[SO_{2(aq)}]$ and its back pressure, reducing the influx of SO_2 (see Eq. 8). The pH is governed in this case by the complex interactions of mass transfer of SO_2, H_2O_2, and NH_3 and the oxidation rate.

The combined effect of mass transfer and chemical equilibrium is more clearly demonstrated with the non-oxidizer, but pH lowering species, HNO_3. HNO_3 and NH_3 have an opposite effect on pH and Figure 17 illustrates how this affects the absorption of SO_2. Plotted are isopleths of absorbed S(IV) as functions of ambient HNO_3 and NH_3 with no oxidizers present. Absorption is decreased by increasing HNO_3 (lowering of pH) and increased by increasing NH_3 (increasing pH). That is, we observe the same phenomenon as previously discussed, only here pH is lowered by HNO_3 and not by an oxidizer.

Effect of Preacidification (100% Conversion)

Raindrops may be acidified prior to entering the polluted zone. Here we assume that occurs and that the raindrops have an initial pH = 4 and SO_4^{2-} = 50 μM prior to entering the polluted zone. The effect on pH and SO_4^{2-} formation for select values of HNO_3, O_3 and H_2O_2 in the presence of $[SO_{2(g)}]$=10 ppb is illustrated in Table III where values of the change in pH and SO_4^{2-} with respect to their initial values are shown. From the table we note the following: (a) preacidification limits further changes in pH and (b) in the presence of H_2O_2, SO_4^{2-} production is independent of preacidification (preacidification does limit SO_4^{2-} production by O_3 oxidation). However we point out that, as the H_2O_2 oxidation rate is explicitly independent of pH, conclusion (a) would no doubt have to be modified somewhat for greater fall heights since, unlike the O_3 oxidation step, H_2O_2 will continue to oxidize S(IV). A fact to note is that a change of pH from 4.6 to 3.6 requires ten times as much hydrogen ions as the change from 5.6 to

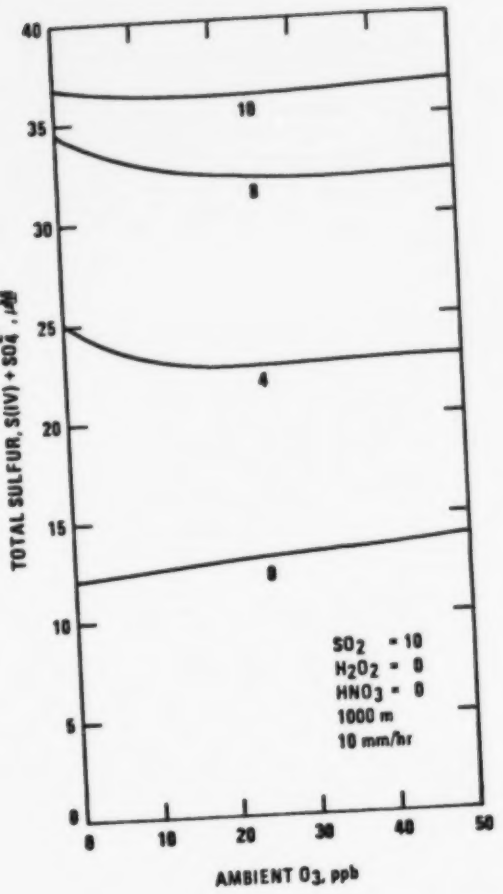
40
35
30
25
20
15
10
5
0
0
10
20
30
40
50
TOTAL SULFUR, S(IV) + SO_4^{2-}, μM
AMBIENT O_3, ppb
18
8
4
0
SO_2 = 10
H_2O_2 = 0
HNO_3 = 0
1000 m
10 mm/hr

13

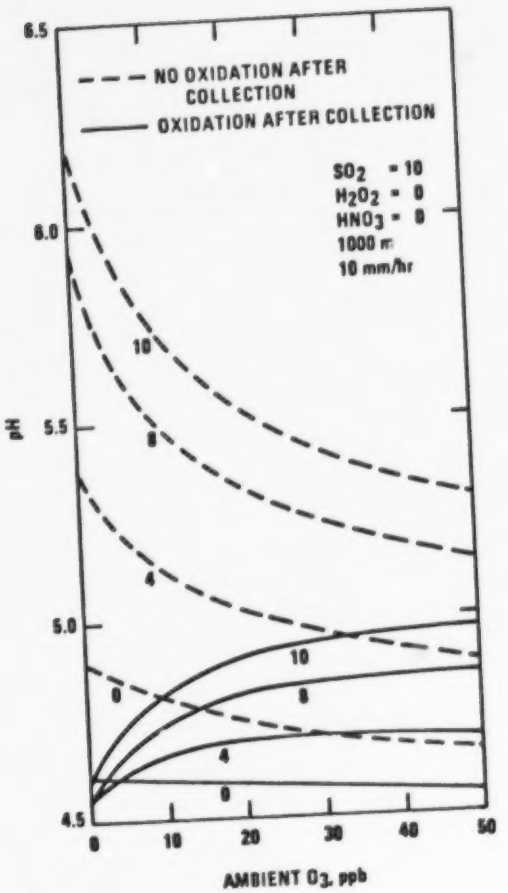
NO OXIDATION AFTER COLLECTION
OXIDATION AFTER COLLECTION
SO_2 = 10
H_2O_2 = 0
HNO_3 = 0
1000 m
10 mm/hr
pH
6.5
6.0
5.5
5.0
4.5
10
8
4
0
10
8
4
0
0
10
20
30
40
50
AMBIENT O_3, ppb

14

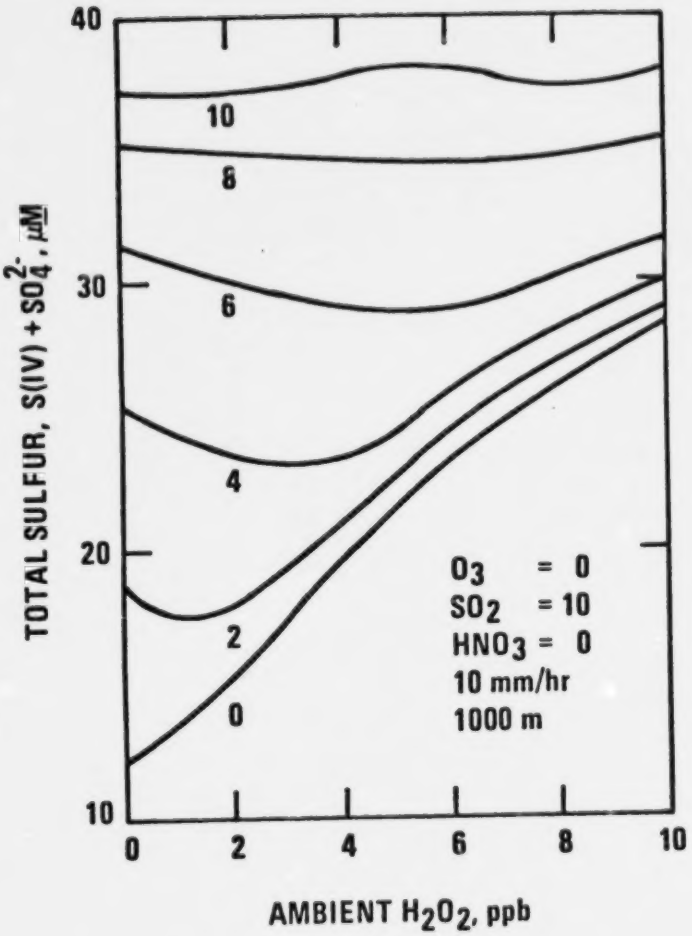
40
30
20
10
0
2
4
6
8
10
10
8
6
4
2
0
O_3 = 0
SO_2 = 10
HNO_3 = 0
10 mm/hr
1000 m
TOTAL SULFUR, S(IV) + SO_4^{2-}, μM
AMBIENT H_2O_2, ppb

15

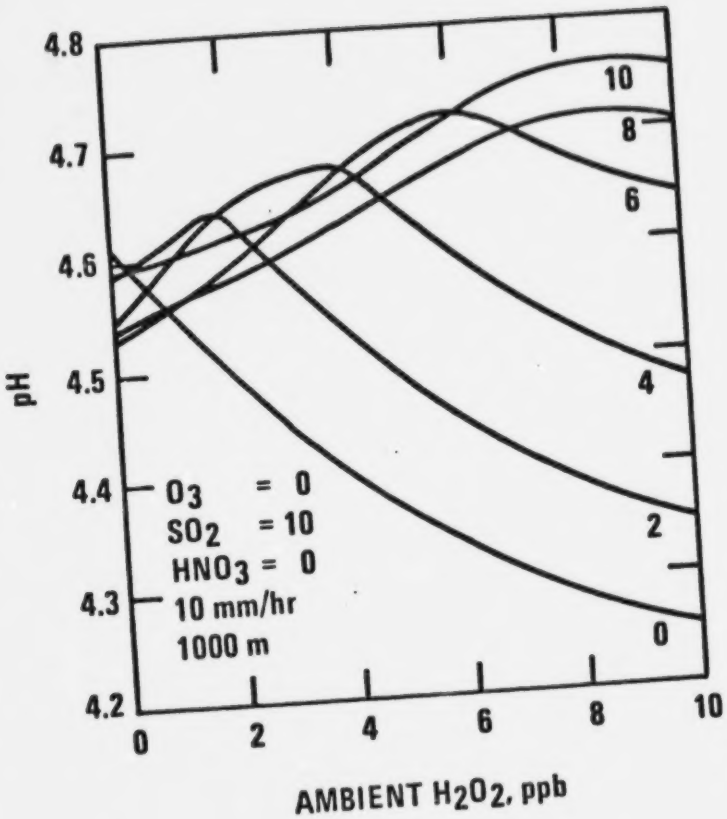
4.8
4.7
4.6
4.5
4.4
4.3
4.2
pH
0
2
4
6
8
10
AMBIENT H_2O_2, ppb
O_3 = 0
SO_2 = 10
HNO_3 = 0
10 mm/hr
1000 m
10
8
6
4
2
0

16

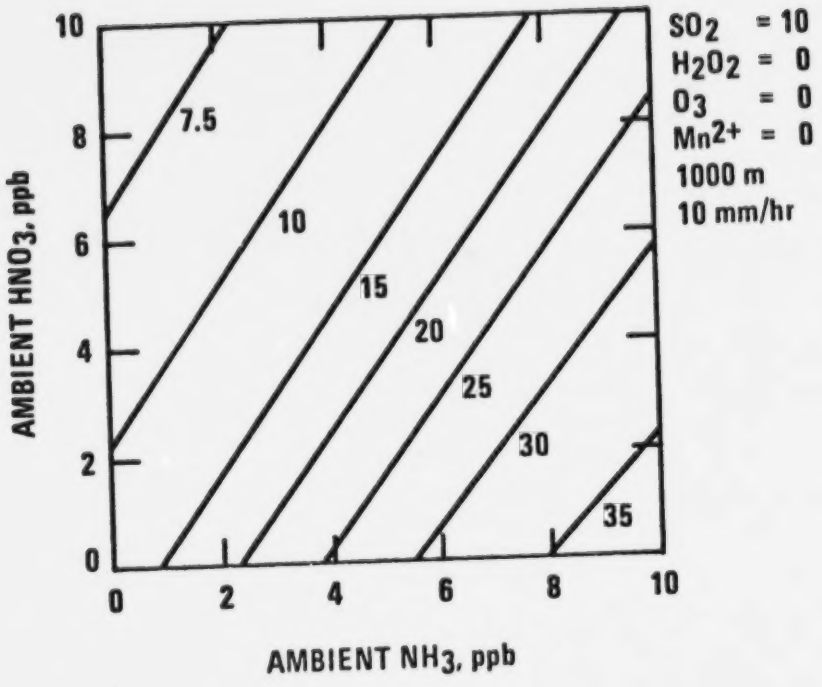
10
8
6
4
2
0
0
2
4
6
8
10
7.5
10
15
20
25
30
35
AMBIENT HNO3, ppb
AMBIENT NH3, ppb
SO2 = 10
H2O2 = 0
O3 = 0
Mn2+ = 0
1000 m
10 mm/hr

17

TABLE IV. EFFECT OF PREACIDIFICATION ([SO_2] = 10 ppb)*

Ambient Concentration, ppb			Case:	pH		SO_4^{2-}, μM	
			Initial:	A 5.6	B 4.0	A 5.6	B 4.0
HNO_3	O_3	H_2O_2		Δ pH	Δ pH	Δ μM	Δ μM
0	0	0		-1.0	0	12	2.0
0	50	0		-1.1	-0.05	14	6.6
10	0	0		-1.4	-0.2	6.4	1.6
10	50	0		-1.4	-0.2	8.6	1.9
0	0	10		-1.4	-0.2	30	26
0	50	10		-1.4	-0.2	32	27
10	0	10		-1.6	-0.3	29	26
10	50	10		-1.7	-0.3	30	27

*Results are from a simulation of (and may apply only to) the idealized rain system model in Figure 2. S(IV) in the collector is assumed to be converted 100% to sulfate. Conditions: Best raindrop distribution; fall height = 1000 m; rain rate = 10 mm/hr., and [$NH_{3(g)}$] = 0.

4.6, and thus, roughly a fall distance 10 times as much as that for a 5.6 to 4.6 pH change. Since the mass transfer rate is limited, the quantity of mass (SO_2, O_3, H_2O_2, etc.) that can be absorbed to produce H^+ is also limited; thus, the effective result of preacidification with respect to pH has the appearance of quenching the reaction.

An Extended Rain Event (No Conversion in Collectors)

In Figures 18 through 22 we illustrate the relationships between rain water concentrations and ambient gas concentrations for simulated 10-mm/hr, 1000-m, 4-hour rain events. Initial conditions are: $[NH_{3(g)}] = [HNO_{3(g)}] = 2$ ppb; $[O_{3(g)}] = 50$ ppb; $[H_2O_{2(g)}] = 5$ ppb with $[SO_{2(g)}]$ the variable parameter from figure to figure beginning with $[SO_{2(g)}] = 2.5$ ppb, then 5 ppb, 10 ppb, 20 ppb, and 40 ppb. Note that no conversion of S(IV) to SO_4^{2-} is effected after collection in these simulations in contrast to most of the simulations discussed here.

There are several observations common to all five figures and we discuss them here. (1) The H_2O_2 sub-cloud scavenging rate is independent of the SO_2 gas phase concentration. Note that after 1 hour $[H_2O_{2(g)}] = 1.5$ ppb regardless of whether the initial $[SO_{2(g)}] = 5$ ppb or 40 ppb. Also the $SO_{2(g)}$ removal rate is much lower than that for $H_2O_{2(g)}$. This is due to the dramatic difference is the Henry's Law constants for the two compounds. (2) As each rain event progresses in time, $[SO_4^{2-}]$ decreases. As the event progresses, $[H_2O_{2(g)}]$ decreases, making less hydrogen peroxide available in the droplets for converting S(IV) to S(VI). In fact at the highest $[SO_{2(g)}]$ we find unreacted S(IV) appearing in the collected rain water, all available $[H_2O_{2(g)}]$ having been already expended in forming SO_4^{2-}. (3) pH gradually increases from t=0 to t=4 hours for all $[SO_{2(g)}]$. As the $[H_2O_{2(g)}]$ decreases, less SO_4^{2-} is being formed (and thus less H^+).

Perhaps the most important observation concerning these five figures concerns the relationship of $[SO_{2(g)}]$, $[H_2O_{2(g)}]$ and $[SO_4^{2-}]$. For convenience we list in Table V selected data from the figures.

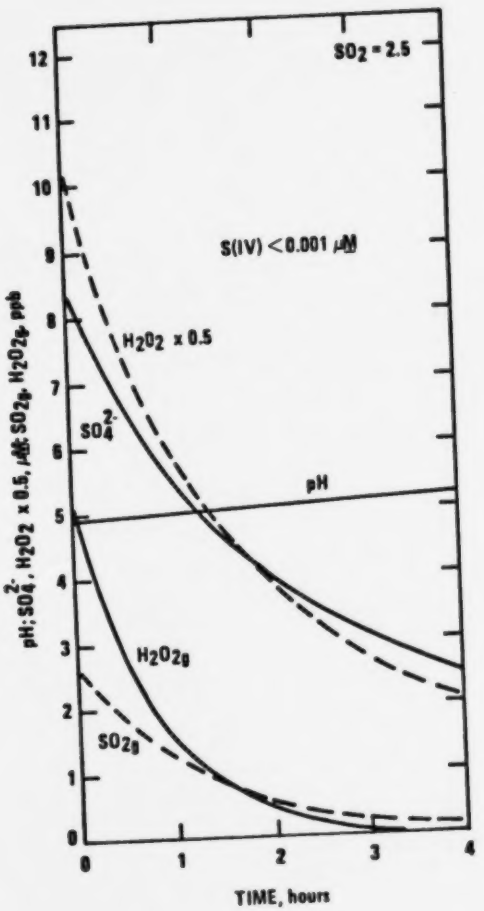
SO_2 = 2.5
S(IV) < 0.001 μM
H_2O_2 x 0.5
SO_4^{2-}
pH
H_2O_{2g}
SO_{2g}
pH; SO_4^{2-}, H_2O_2 x 0.5, μM; SO_{2g}, H_2O_{2g}, ppb
TIME, hours

18

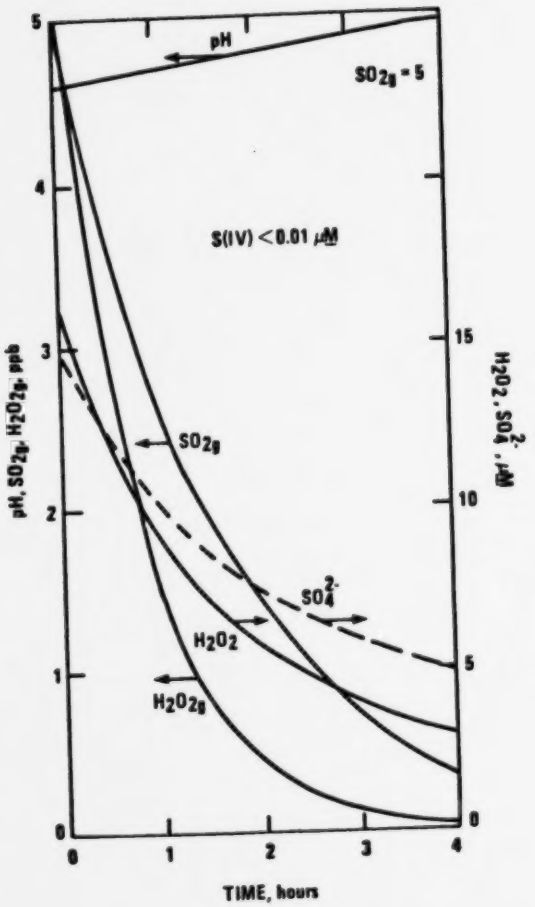
pH
SO_{2g} = 5
S(IV) < 0.01 μM
SO_{2g}
SO_4^{2-}
H_2O_2
H_2O_{2g}
pH, SO_{2g}, H_2O_{2g}, ppb
H_2O_2, SO_4^{2-}, μM
TIME, hours
0
1
2
3
4
5
15
10

19

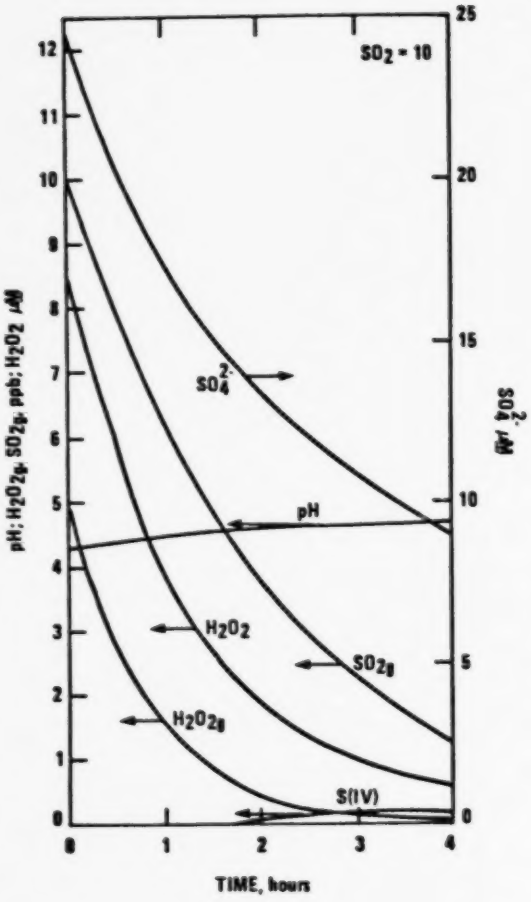
SO_2 = 10
SO_4^{2-}
pH
H_2O_2
SO_{2g}
H_2O_{2g}
S(IV)
pH; H_2O_{2g}, SO_{2g}, ppb; H_2O_2 μM
SO_4^{2-} μM
TIME, hours

20

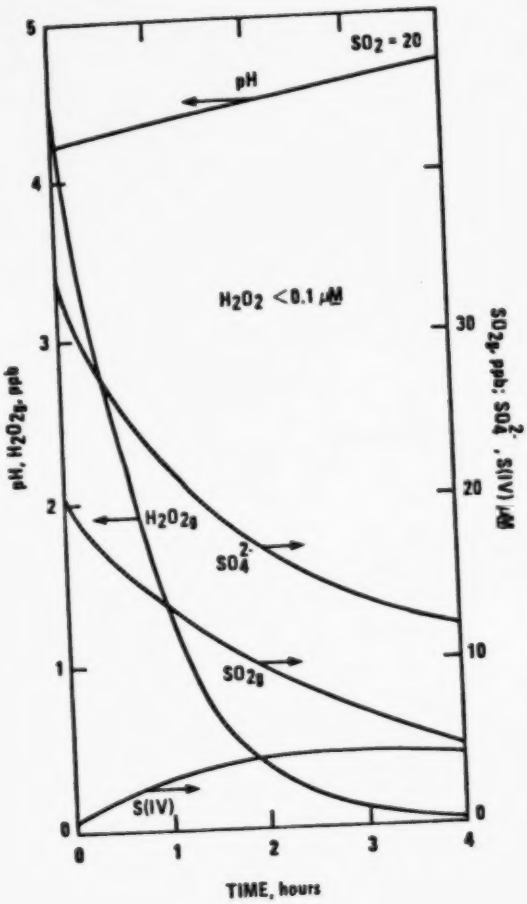
SO_2 = 20
pH
H_2O_2 <0.1 μM
H_2O_2
SO_4^{2-}
SO_2
S(IV)
pH, H_2O_2, ppb
SO_2, ppb; SO_4^{2-}, S(IV) μM
TIME, hours
0
1
2
3
4
5
10
20
30

21

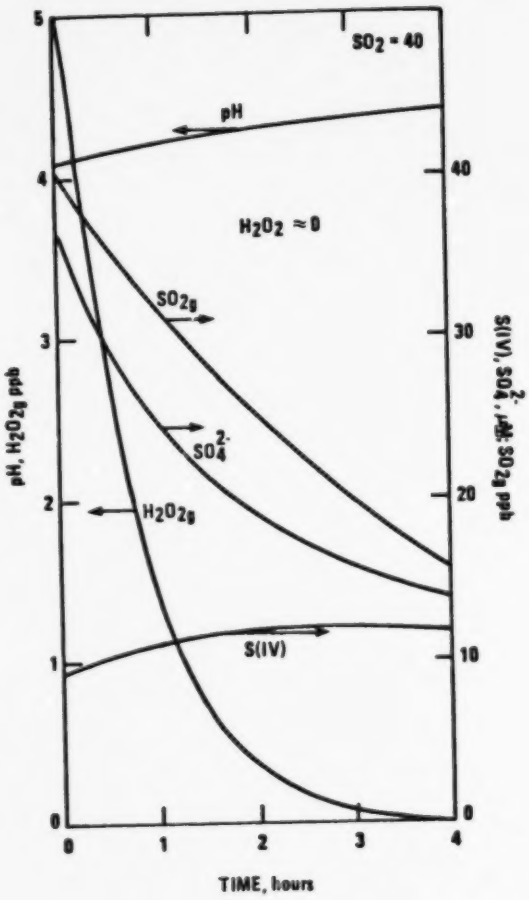
SO_2 = 40
pH
$H_2O_2 \approx 0$
SO_{2g}
SO_4^{2-}
H_2O_{2g}
S(IV)
pH, H_2O_{2g} ppb
S(IV), SO_4^{2-}, SO_{2g} ppb
TIME, hours
0
1
2
3
4
5
10
20
30
40

22

TABLE V. SULFATE CONCENTRATION IN RAIN AT 1 AND AT 4 HOURS AFTER START OF EVENT.*

$[SO_{2(g)}]_i$	Time,hr:	$[SO_4^{2-}]$, μM	
		1	4
2.5		5.7	2.3
5.0		10	5
10		17	9
20		21	12
40		25	12

*Results are from a simulation of (and may apply only to) the idealized rain system model in Figure 2. S(IV) in the collector is assumed to be converted 100% to sulfate. Conditions: Best raindrop distribution; fall distance = 1000 m; rain rate = 10 mm/hr.; $[H_2O_{2(g)}]_i$ = 5 ppb; $[NH_{3(g)}]_i$ = 2 ppb; and $[HNO_{3(g)}]_i$ = 2 ppb.

As can be seen by these individual values from each of the five figures, $[SO_{2(g)}]_i/[H_2O_{2(g)}]_i$ determines the functional relationship of $[SO_{2(g)}]_i$ to $[SO_4^{2-}]$ in the rain. If $[SO_{2(g)}] \gg [H_2O_{2(g)}]$, as is the case for the last two rows, then the relationship is non-linear. A 50% reduction in $[SO_{2(g)}]$ from 40 ppb to 20 ppb does not result in a simular reduction in SO_4^{2-}, regardless of the duration of the rain ($t < 4$ hr.). However, if $[SO_{2(g)}] \sim [H_2O_{2(g)}]$, then a linear relationship is observed. In that instance, a 50% reduction in $[SO_{2(g)}]$ from 5 ppb to 2.5 ppb does result in a comparable $[SO_4^{2-}]$ reduction in the rain water.

As was pointed out in the Introduction, this model lacks many of the necessary features for simulating real events of interest. However, the simulations using this model suggest that rain acidification is a complex process and that strategies for improvement should consider both oxidant and SO_2 controls.

Effect of Rain Rate, Fall Distance and Raindrop Distribution

As the rain rate decreases, the peaks of the raindrop distributions shift towards drops of smaller radii (Figure 2). Since the mass transfer coefficient is inversely proportional to the radius, the influx of material per unit volume of drop is larger for smaller drops. Table 5 illustrates the effect for two rain rates, 1 mm/hr and 10 mm/hr. The concentrations for the species H^+, SO_4^{2-}, NO_3^-, and NH_4^+ are 2 to 2.5 times as large for the 1 mm/hr rate as for the 10 mm/hr rate. On the other hand the total quantity of a species absorbed is less (by a factor of 0.2 - 0.25 for the same length of time) for the smaller rain rates.

Increased fall distance increases the amount of pollutant absorbed and products created. As illustrated in Table VI, an increase from 1000 m to 3000 m increases $[H^+]$, $[SO_4^{2-}]$, $[NO_3^-]$, and $[NH_4^+]$ by a factor of 3, which is the ratio of the fall heights. (H_2O_2 is removed by oxidizing S(IV); however, total absorbed H_2O_2 is about 3 times as much for the higher fall distance.) The absorption of HNO_3 and NH_3 is limited by mass transfer, due to their low Henry's law constants and the transformation to NO_3^- and NH_4^+; their back pressures are insignificant. The quantity absorbed (mostly in the form NO_3^- and NH_4^+) are thus proportional to fall distance. For the conditions in Table VI, the quantities of SO_2 absorption are also about 3 times as much for the longer fall distance; this is because there is sufficient H_2O_2 to oxidize the dissolved SO_2 and make its back pressure insignificant. Thus, the production of total S_T is proportional to height; however, this value is much more dependent on the ambient concentrations of gases such as H_2O_2 than are the values for NO_3^- and NH_4^+.

The Best and Marshall-Palmer raindrop size distributions are illustrated with their density functions (fraction of water/unit radius) for two rain rates in Figure 2. The main difference between the two distributions (for radii > 0.1 mm) is that there is more water at smaller radii for the Marshall-Palmer distribution. Thus we can expect a higher concentration of species, for the same rain rate, using the Marshall-Palmer distribution. In our simulations this distribution produced up to 50% more chemical products than the Best distribution did. However, it is difficult to know if there is any meaning to the quantitative differences between the two distributions. For example, Marshall and Palmer state that their distribution overestimates the number of drops with radii below about 0.6 mm, which is a region in which there is significant quantity of

TABLE VI. INFLUENCE OF SIZE DISTRIBUTION ON COMPOSITION OF COLLECTED RAIN*

Fall Distance, meters	Rain Rate, mm/hr	pH	$[S_T] = [SO_4^{2-}]$, μM	$[NO_3^-]$, μM	$[NH_4^+]$, μM	$[H_2O_2]$, μM
BEST DISTRIBUTION						
1000	1	4.10	54.6	58.4	87.3	22.2
1000	10	4.41	24.9	22.5	33.4	12.2
3000	1	3.58	174	175	262	28.4
3000	10	3.95	72.4	67.4	100	16.5
MARSHALL - PALMER DISTRIBUTION						
1000	1	3.97	73.8	81.6	123	27.8
1000	10	4.29	33.3	32.6	48.5	15.8
3000	1	3.45	240	245	368	34.2
3000	10	3.81	102	97.9	146	21.0

*Results are from a simulation of (and may apply only to) the idealized rain system model shown in Figure 2. S(IV) in the collector is assumed to be converted 100% to sulfate. Initial conditions:

$[O_{3(g)}] = 50$ ppb $\qquad [NH_{3(g)}] = 5$ ppb

$[H_2O_{2(g)}] = 5$ ppb $\qquad [SO_{2(g)}] = 10$ ppb

$[HNO_{3(g)}] = 5$ ppb $\qquad [Mn^{2+}] = 5$ μM

water. This might suggest that the Best distribution is better. Also, we limit drop sizes to radius > 0.1 mm; what is the effect of drops below this size? On the positive side both distributions give rise to the same qualitative response to changes in rain rate and fall distance: a decrease in rain rate and an increase in fall distance increase absorption. In fact, as illustrated in Table VII, the ratio of concentrations due to one rain rate to another or due to concentrations at one fall height to concentrations at another indicate considerable similarity between the two distributions as far as these results are concerned. Although it may be premature (without more simulations along these lines) there is evidence here that qualitative conclusions concerning the nature of below cloud scavenging, as simulated by our model, do not depend on which of the two rain drop distributions we use.

TABLE VII. COMPARISON OF RATIOS OF CONCENTRATIONS FOR THE BEST AND MARSHALL - PALMER DISTRIBUTIONS AS A FUNCTION OF RAIN RATE AND FALL DISTANCES.*

Effect of Decreasing		Ratio of Concentrations[a]									
		Δ pH[b]		S_T		NO_3^-		NH_4^+		H_2O_2	
		B[c]	MP[d]	B	MP	B	MP	B	MP	B	MP
A. Rain rates from 10 mm/hr to 1 mm/hr	z = 1 km:	-0.31	-0.32	0.46	0.45	0.39	0.40	0.38	0.39	0.55	0.57
	3 km:	-0.37	-0.36	0.42	0.42	0.38	0.40	0.38	0.40	0.58	0.60
B. Fall distance from 3 km to 1 km	p = 1 mm/hr:	-0.52	-0.52	3.19	3.25	3.00	3.00	3.00	2.99	1.28	1.23
	10 mm/hr:	-0.52	-0.48	2.91	3.00	3.00	3.00	2.99	3.01	1.35	1.33

*The results are from a simulation of (and may apply only to) the idealized rain system model shown in Figure 2. S(IV) in the collector is assumed to be converted 100% to sulfate.

a. Ratio: $[s]_i/[s]_j$ where i = 10 mm/hr or 3 km
j = 1 mm/hr or 1 km, respectively

b. Δ pH = $pH_i - pH_j$

c. B = Best distribution

d. MP = Marshall - Palmer distribution

CONCLUSIONS

The simulations using the sub-cloud scavenging/chemical reaction model indicate that :

1. H_2O_2 is a more effective oxidizer of dissolved SO_2 than are O_3, Mn^{2+}, and C(O).

2. The rate of acidification is non-linear with respect to the concentration of SO_2 when $[SO_{2(g)}] > [H_2O_{2(g)}]$. A reduction of SO_2 concentration for this case does not reduce the rate or quantity of sulfuric acid formed, as long as $[SO_{2(g)}] > [H_2O_{2(g)}]$. If $[SO_{2(g)}] < [H_2O_{2(g)}]$, then a reduction in $[SO_{2(g)}]$ will yield a proportional reduction in formation of sulfuric acid in the rain.

3. HNO_3 inhibits the effectiveness of O_3 for oxidizing dissolved SO_2. For pH < 6, it appears that this reaction is not important if $[H_2O_{2(g)}]$ is greater than about 1 ppb. The effectiveness of H_2O_2 for oxidizing dissolved SO_2 is not inhibited over the range 2 < pH < 6; the absorption of HNO_3 does not decrease the rate of formation of sulfuric acid.

4. HNO_3 is rapidly scavenged by the initial rain fall, and it is likely responsible for the lower values of pH observed at the beginning of a rain.

5. H_2O_2 is also rapidly scavenged. The collection of the initial rain with high concentrations of dissolved H_2O_2 is an important consideration for the subsequent oxidation of dissolved SO_2 delivered to the collector in the latter part of the rain (with higher pH and less scavenged H_2O_2). The wet deposition of H_2O_2, especially in the initial rain fall, must be regarded as an acidifying agent that can react with either wet-deposited SO_2 or naturally occurring S(II), S(IV), N(III) and organic compounds to produce acids.

6. The model indicated equivalent results for the chemical composition of collected rain for the Best and the Marshall - Palmer rain drop size

distributions for the specific conditions that we have used (precipitation rates of 1 mm/hr and 10 mm/hr; fall distances of 1 km and 3 km).

There are recent advances in the awareness of the roles of possible inhibitors of the H_2O_2 oxidation of dissolved SO_2, especially by formaldehyde. Presently, there is insufficient knowledge of the kinetics of that reaction and the concentration range of formaldehyde for us to include it in the simulations. Additional refinements to be added to the model include the the temperature dependence of the Henry's law values and chemical kinetics.

NOTATION

A	surface area of drop
C	pointwise concentration
C_A	pointwise concentration of a chemical species on the liquid phase side of the surface of the drop
D	diffusion coefficient, cm^2/sec
H	Henry's law constant, dimensionless. Equilibrium ratio of gas phase to aqueous phase concentration of the same species.
N	number of chemical species
R	drop radius, mm
Sh	Sherwood number
g	indicates gas phase
i	rate constant subscript, reaction equation number
k_g	gas phase mass transfer coefficient, cm/sec
$\underline{M}$	moles/liter
p	precipitation rate, mm/hr
s	indicates a chemical species, such as SO_2
t	time
u	fall velocity, m/sec
V	volume of drop
z	fall distance, m
$[\ ]$	molar concentration
ν	kinematic viscosity of air, 0.133 cm^2/sec
Γ	chemical reaction rate
$\underline{v}$	medium velocity
r	unit radius vector
$\overline{f}$	overbar indicates volume average of a function, f
$\underline{f}$	underbar indicates a vector of function, f
ρ	average ground level concentration
$\oint\!\!\!\oint$	integral over surface of drop

APPENDIX

Presented here is the set of differential equations used for the chemical kinetics in the aqueous droplets. All concentrations are for the liquid phase, unless denoted with a subscript "g" (gas phase). The value of the mass transfer coefficient, k_g, and Henry's law constant, H, depend on the species.

$$ud[i]/dz\Big|_{Mn(II)} = \text{rate of change of species i due to the Mn(II) catalytic oxidation reaction}$$

$$= ud[SO_4^{2-}]/dz\Big|_{Mn(II)} = -ud[HSO_3^-]/dz\Big|_{Mn(II)}$$

$$= (1.45\times10^{+5})[HSO_3^-]^{1.5}[Mn(II)].$$

$$ud[H^+]/dz = -k_{-1}[H^+][OH^-] + K_{+1} + k_{+2}[CO_2] - k_{-2}[H^+][HCO_3^-] + k_{+4}[SO_2] - k_{-4}[H^+][HSO_3^-] + k_{+5}[HSO_3^-] - [H^+][SO_3^{2-}] + k_{+6}[HNO_3] - k_{-6}[H^+][NO_3^-] + k_{+7}[NH_4^+] - k_{-7}[NH_3][H^+] + k_{11}[O_3][HSO_3^-] + 2k_{12}[H_2O_2][SO_2] + ud[H^+]/dz\Big|_{Mn(II)}.$$

$$ud[OH^-]/dz = K_{+1} - k_{-1}[H^+][OH^-] - k_{-3}[CO_2][OH^-] + k_{-3}[HCO_3^-] + k_{-8}[NH_3] - k_{-8}[NH_4^+][OH^-].$$

$$ud[CO_2]/dz = -k_{+2}[CO_2] + k_{-2}[H^+][HCO_3^-] - k_{-3}[CO_2][OH^-] + k_{+3}[HCO_3^-] + (30k_g/R)([CO_{2(g)}] - H[CO_2]).$$

$$u[HCO_3^-]/dz = +k_{+2}[CO_2] - k_{-2}[HCO_3^-][H^+] + k_{-3}[CO_2][OH^-] - k_{+3}[HCO_3^-].$$

$$ud[SO_2]/dz = -k_{+4}[SO_2] + k_{-4}[H^+][HSO_3^-] - [SO_2](k_9[O_3] + k_{12}[H_2O_2]) + (30k_g/R)([SO_{2(g)}] - H[SO_2]).$$

$$ud[HSO_3^-]/dz = k_{+4}[SO_2] - k_{-4}[H^+][HSO_3^-] - k_{-5}[HSO_3^-] + k_{+5}[SO_3^{2-}] + ud[HSO_3^-]\Big|_{Mn(II)}.$$

$$ud[SO_3^{2-}]/dz = k_{+5}[HSO_3^-] - k_{-5}[SO_3^{2-}][H^+] - k_{10}[O_3][SO_3^{2-}].$$

APPENDIX

Presented here is the set of differential equations used for the chemical kinetics in the aqueous droplets. All concentrations are for the liquid phase, unless denoted with a subscript "g" (gas phase). The value of the mass transfer coefficient, k_g, and Henry's law constant, H, depend on the species.

$$ud[i]/dz\Big|_{Mn(II)} = \text{rate of change of species i due to the Mn(II) catalytic oxidation reaction}$$

$$= ud[SO_4^{2-}]/dz\Big|_{Mn(II)} = -ud[HSO_3^-]/dz\Big|_{Mn(II)}$$

$$= (1.45\times10^{+5})[HSO_3^-]^{1.5}[Mn(II)].$$

$$ud[H^+]/dz = -k_{-1}[H^+][OH^-] + k_{+1} + k_{+2}[CO_2] - k_{-2}[H^+][HCO_3^-] + k_{+4}[SO_2] - k_{-4}[H^+][HSO_3^-] + k_{+5}[HSO_3^-] - k_{-5}[H^+][SO_3^{2-}] + k_{+6}[HNO_3] - k_{-6}[H^+][NO_3^-] + k_{+7}[NH_4^+] - k_{-7}[NH_3][H^+] + k_{11}[O_3][HSO_3^-] + 2k_{12}[H_2O_2][SO_2] + ud[H^+]/dz\Big|_{Mn(II)}.$$

$$ud[OH^-]/dz = k_{+1} - k_{-1}[H^+][OH^-] - k_{-3}[CO_2][OH^-] + k_{-3}[HCO_3^-] + k_{-8}[NH_3] - k_{-8}[NH_4^+][OH^-].$$

$$ud[CO_2]/dz = -k_{+2}[CO_2] + k_{-2}[H^+][HCO_3^-] - k_{-3}[CO_2][OH^-] + k_{+3}[HCO_3^-] + (30k_g/R)([CO_{2(g)}] - H[CO_2]).$$

$$u[HCO_3^-]/dz = +k_{+2}[CO_2] - k_{-2}[HCO_3^-][H^+] + k_{-3}[CO_2][OH^-] - k_{+3}[HCO_3^-].$$

$$ud[SO_2]/dz = -k_{+4}[SO_2] + k_{-4}[H^+][HSO_3^-] - [SO_2](k_9[O_3] + k_{12}[H_2O_2]) + (30k_g/R)([SO_{2(g)}] - H[SO_2]).$$

$$ud[HSO_3^-]/dz = k_{+4}[SO_2] - k_{-4}[H^+][HSO_3^-] - k_{-5}[HSO_3^-] + k_{+5}[SO_3^{2-}] - k_{11}[O_3][SO_3^-] + ud[HSO_3^-]\Big|_{Mn(II)}.$$

$$ud[SO_3^{2-}]/dz = k_{+5}[HSO_3^-] - k_{-5}[SO_3^{2-}][H^+] - k_{10}[O_3][SO_3^{2-}].$$

$$ud[O_3]/dz = -[O_3](k_9[SO_2] + k_{10}[SO_3^{2-}] + k_{11}[HSO_3^-]) + (30k_g/R)([O_{3(g)}] - H[O_3]).$$

$$ud[SO_4^{2-}]/dz = [O_3](k_9[SO_2] + k_{10}[SO_3^{2-}] + k_{11}[HSO_3^-]) + ud[SO_4^{2-}]\Big|_{Mn(II)} + k_{12}[H_2O_2][SO_2].$$

$$ud[HNO_3]/dz = -k_{+6}[HNO_3] + k_{-6}[H^+][NO_3^-] + (30k_g/R)([HNO_{3(g)} - H[HNO_3]).$$

$$ud[NO_3^-]/dz = k_{+6}[HNO_3] - k_{-6}[H^+][NO_3^-].$$

NOTATION

D	diffusion coefficient, cm^2/sec
H	Henry's law constant, dimensionless. Equilibrium ratio of gas phase concentration to liquid phase concentration of same species
R	drop radius, mm
g	indicates gas phase
i	rate constant subscript, reaction equation number
k_g	gas phase mass transfer coefficient, cm/sec
k_{+1}, k_{-1}	toward backward rate constant for the ith reaction
l	liter
m	meter
mm	millimeter
s	indicates a chemical species such as SO_2, HNO_3, H^+, HSO_3^-, etc.
t	time
u	fall velocity, m/sec
z	fall distance, meters
P	indicates liquid phase
	molar concentration
n	kinematic viscosity of air, 0.133 cm^2/sec
mm	10^{-6} moles/liter
A	gradient vector
A^2	Laplacian
Q	chemical reaction rate
$\underline{v}$	medium velocity
V	volume of a raindrop
r	unit radius vector
$\bar{f}$	overbar indicates volume average of a function, f
$\iint_A$	integral over drop surface

dA	element of surface area
C	pointwise concentration of a chemical species
C_A	pointwise concentration of a chemical species on the liquid phase side of the surface of a drop
Sh	Sherwood number
$\underline{C}$	underbar indicates a vector of functions
N	number of chemical species

CAPTIONS

Figure No.	
1	Rain System Model. The raindrops form above and fall through a polluted zone where they absorb reactive gases, producing H^+, SO_4^{2-}, NO_3^-, and other species.
2	The Marshall - Palmer and the Best Raindrop Size Density (Fraction of Water) Functions for Two Precipitation Rates. Note the shift towards smaller drop sizes in both distributions for a decrease in the precipitation rate.
3	The Effect of Ambient SO_2 and Specific Oxidizing Systems on the Production of Total Sulfur (S_T) or SO_4^{2-} in the Presence of $[HNO_3]$ = 5 ppb. The data are from a simulation of (and may apply only to) the idealized rain system model shown in Figure 2. S(IV) in the collector is assumed to be converted 100% to SO_4^{2-}. Conditions: Best raindrop distribution; fall distance = 1000 m; rain rate = 10 mm/hr; initial pH = 5.63. The units of concentration for the gas phase pollutants are in ppb; the units of concentration of Mn^{2+} and SO_4^{2-} in the rain water are in $\mu\underline{M}$.
4	The Effect of Ambient H_2O_2 and O_3 on pH and $[SO_4^{2-}]$ in Rain. Plotted are isopleths of the resulting pH (solid curves) and $[SO_4^{2-}]$ (broken curves) for ambient values of $[H_2O_2]$ and $[O_3]$. The data are from a simulation of (and may only apply to) the idealized rain system model shown in Figure 2. S(IV) in the collector is assumed to be converted 100% to SO_4^{2-}. Conditions: Best raindrop distribution; fall distance = 1000 m; rain rate = 10 mm/hr.; initial raindrop pH = 5.63; ambient $[SO_2]$ = 10 ppb, ambient $[HNO_3]$ = 0 ppb. The units of concentration of SO_4^{2-} in the rain water are $\mu\underline{M}$.

5. The Effect of Ambient H_2O_2 and HNO_3 on pH, $[SO_4^{2-}]$, and $[NO_3^-]$ in Rain. Plotted are isopleths of pH (dotted curves), $[SO_4^{2-}]$ (broken curves), and the ratio $[NO_3^-]/[SO_4^{2-}]$ (solid curves). The data are from a simulation of (and may only apply to) the idealized rain system model shown in Figure 2. S(IV) in the collector has been assumed to be converted 100% to SO_4^{2-}. Conditions: Best raindrop distribution; fall distance = 1000 m; rain rate = 10 mm/hr.; initial rain water pH = 5.63; ambient $[O_3]$ = 50 ppb; ambient $[SO_2]$ = 10 ppb. The units of $[SO_4^{2-}]$ are $\mu\underline{M}$.

6. The Efect of Ambient H_2O_2 and HNO_3 on pH, Sulfate, and Nitrate in Rain. Plotted are isopleths of pH (dotted curves), $[SO_4^{2-}]$ (broken curves), and the ratio $[NO_3^-]/[SO_4^{2-}]$ (solid curves). The data are from a simulation of (and may apply only to) the idealized rain system model shown in Figure 2. S(IV) in the collector has been assumed to be converted 100% to SO_4^{2-}. Conditions: Best raindrop distribution; fall distance = 1000 m; rain rate = 10 mm/hr.; initial rain water pH = 5.63; $[O_{3(g)}]$ = 50 ppb; and, $[SO_{2(g)}]$ = 20 ppb. The units of $[SO_4^{2-}]$ are $\mu\underline{M}$.

7. The Effect of Ambient SO_2 and HNO_3 on pH, SO_4^{2-}, and NO_3^- in Rain. Plotted are isopleths of pH (dotted curves), $[SO_4^{2-}]$ (broken curves), and the ratio $[NO_3^-]/[SO_4{}^{2-}]$ (solid curves). The data are from a simulation of (and may apply only to) the idealized rain system model shown in Figure 2. S(IV) in the collector has been assumed to be converted 100% to SO_4^{2-}. Note that the absorption of HNO_3 by the falling droplets lowers the pH and retards the reaction between dissolved SO_2 and O_3 to form SO_4^{2-}. Conditions: Best raindrop distribution; fall distance = 1000 m; rain rate = 10 mm/hr.; initial rain water pH

= 5.63; $[O_{3(g)}]$ = 50 ppb; and $[H_3O_{2(g)}]$ = 0 ppb. The units of $[SO_4^{2-}]$ are μM.

8. The Effect of Ambient SO_2 and HNO_3 on pH, SO_4^{2-}, and NO_3^- in the Presence of H_2O_2. Plotted are isopleths of pH (dotted curves), $[SO_4^{2-}]$ (broken curves) and the ratio $[NO_3^-]/[SO_4^{2-}]$ (solid curves). The data are from a simulation of (and may apply only to) the idealized rain system model shown in Figure 2. S(IV) in the collector has been assumed to be converted 100% to SO_4^{2-}. Note that the absorption of HNO_3 by the falling droplets lowers the pH and slightly retards the formation of SO_4^{2-}. Conditions: Best rain drop distribution; fall distance = 1000 m; rain rate = 10 mm/hr.; initial rain water pH = 5.63; $[O_{3(g)}]$ = 50 ppb; and $[H_2O_{2(g)}]$ = 10 ppb. The units of $[SO_4^{2-}]$ are μM.

9. Isopleths of pH as a Function of Ambient H_2O_2 and SO_2. The data are from a simulation of (and may apply only to) the idealized rain system model shown in Figure 2. S(IV) in the collector has been assumed to be converted 100% to SO_4^{2-}. Conditions: Best raindrop distribution; fall distance = 1000 m; rain rate = 10 mm/hr.; initial rain water pH = 5.63; $[HNO_{3(g)}] = [NH_{3(g)}] = [O_{3(g)}]$ = 0 ppb; $[Mn^{2+}]$ = 0 μM.

10. Isopleths of pH as a Function of Ambient H_2O_2 and SO_2. The data are from a simulation of (and may apply only to) the idealized rain system model shown in Figure 2. S(IV) in the collector has been assumed to be converted 100% to SO_4^{2-}. Conditions: Same as for Figure 9, except that $[HNO_{3(g)}]$ = 5 ppb.

11. Isopleths of S_T (Total Sulfur Concentration as S(IV) and S(VI)) as a Function of Ambient H_2O_2 and SO_2. The data are from a simulation of (and may apply only to) the idealized rain system model shown in Figure 2. Conditions: Same as for Figure 9. The units of $[S_T]$ are μM.

12. Isopleths of S_T (Total Sulfur Concentration as S(IV) and S(VI)) as a Function of Ambient H_2O_2 and SO_2. The data are from a simulation of (and may apply only to) the idealized rain system model shown in Figure 2. Conditions: Same as for Figure 9, except that $[HNO_{3(g)}]$ = 5 ppb. The units of $[S_T]$ are μM.

13. The Absorption of S_T as a Function of $[O_{3(g)}]$ for Four Values of $[NH_{3(g)}]$: 0, 4, 8, and 10 ppb. The data are from a simulation of (and may apply only to) the idealized rain system model shown in Figure 2. Conditions: Best raindrop distribution; fall distance = 1000 m; rain rate = 10 mm/hr.; initial rain water pH = 5.63; $[SO_{2(g)}]$ = 10 ppb; and $[H_2O_{2(g)}] = [HNO_{3(g)}]$ = 0 ppb. Note that for $[NH_{3(g)}] > 0$, S_T decreases with increasing $[O_{3(g)}]$.

14. The Effect on pH of the Complete Oxidation of S(IV) to SO_4^{2-} After Collection as a Function of Ambient $[O_{3(g)}]$ for Four Values of $[NH_{3(g)}]$: 0, 4, 8, and 10 ppb. The behavior for no conversion of S(IV) in the collector to SO_4^{2} (broken curves) is contrasted to 100% conversion (solid curves) in the collector. The data are from a simulation of (and may apply only to) the idealized rain system model shown in Figure 2. Conditions: Best raindrop distribution; fall distance = 1000 m; rain rate = 10 mm/hr.; initial rain water pH = 5.63; $[SO_{2(g)}]$ = 10 ppb; and $[H_2O_{2(g)}] = [HNO_{3(g)}]$ = 0 ppb.

15. The Content of S_T in Rain Water as a Function of $[H_2O_{2(g)}]$ for Six Values of $[NH_{3(g)}]$: 0, 2, 4, 8, 10 ppb. The data are from a simulation of (and may apply only to) the idealized rain system model shown in Figure 2. Conditions: Best raindrop distribution; fall distance = 1000 m; rain rate = 10 mm/hr.; initial rain water pH = 5.63; $[SO_{2(g)}]$ = 10 ppb; and $[O_{3(g)}]$ = $[HNO_{3(g)}]$ = 0 ppb.

16. pH as a Function of Ambient H_2O_2 for Six Values of Ambient $[NH_{3(g)}]$: 0, 2, 4, 6, 8, 10 ppb. The data are from a simulation of (and may apply only to) the idealized rain system model shown in Figure 2. S(IV) in the collector is assumed to be converted 100% to SO_4^{2-}. Conditions: Best raindrop distribution; fall distance = 1000 m; rain rate = 10 mm/hr.; initial rain water pH = 5.63; $[SO_{2(g)}]$ = 10 ppb; and $[O_{3(g)}]$ = $[HNO_{3(g)}]$ = 0 ppb.

17. Isopleths of $[S_T]$ as Function of $[NH_{3(g)}]$ and $[HNO_{3(g)}]$. The data are from a simulation of (and may apply only to) the idealized rain system model shown in Figure 2. S(IV) in the collector is assumed to be converted 100% to SO_4^{2-}. Conditions: Best raindrop distribution; fall distance = 1000 m; rain rate = 10 mm/hr.; initial rain water pH = 5.63; $[SO_{2(g)}]$ = 10 ppb; $[H_2O_{2(g)}]$ = $[O_{3(g)}]$ = 0 ppb; and $[Mn^{2+}]$ = 0 $\mu\underline{M}$. Note that increasing $[NH_{3(g)}]$ increases the uptake of SO_2 and the $[S_T]$, and $[HNO_{3(g)}]$ causes it to decrease.

18. $[SO_{2(g)}]$ = 2.5 ppb: Concentration of Various Ambient and Liquid Phase Species as a Function of Time for a 4-Hour Rain Event. The data are from a simulation of (and may apply only to) the idealized rain system model shown in Figure 2. No conversion of S(IV) to SO_4^{2-} is assumed to occur in the collector. Conditions: Best raindrop distribution; fall distance = 1000 m; rain rate = 10 mm/hr.; initial rain water pH = 5.63; $[SO_{2(g)}]$ = 2.5 ppb; $[NH_{3(g)}]$ = $[HNO_{3(g)}]$ = 2 ppb; $[O_{3(g)}]$ = 50 ppb; and $[H_2O_{2(g)}]$ = 5 ppb.

19. $[SO_{2(g)}]$ = 5.0 ppb: Concentration of Various Ambient and Liquid Phase Species as a Function of Time for a 4-Hour Rain Event. The data are from a simulation of (and may apply only to) the idealized rain system model shown in Figure 2. No conversion of S(IV) to SO_4^{2-} is assumed to occur in the collector. Conditions: Best raindrop distribution; fall distance = 1000 m; rain rate = 10 mm/hr.; initial rain water pH = 5.63; $[SO_{2(g)}]$ = 5.0 ppb; $[NH_{3(g)}]$ = $[HNO_{3(g)}]$ = 2 ppb; $[O_{3(g)}]$ = 50 ppb; and $[H_2O_{2(g)}]$ = 5 ppb.

20. $[SO_{2(g)}]$ = 10.0 ppb: Concentration of Various Ambient and Liquid Phase Species as a Function of Time for a 4-Hour Rain Event. The data are from a simulation of (and may apply only to) the idealized rain system model shown in Figure 2. No conversion of S(IV) to SO_4^{2-} is assumed to occur in the collector. Conditions: Best raindrop distribution; fall distance = 1000 m; rain rate = 10 mm/hr.; initial rain water pH = 5.63; $[SO_{2(g)}]$ = 10.0 ppb; $[NH_{3(g)}]$ = $[HNO_{3(g)}]$ = 2 ppb; $[O_{3(g)}]$ = 50 ppb; and $[H_2O_{2(g)}]$ = 5 ppb.

21. $[SO_{2(g)}]$ = 20.0 ppb: Concentration of Various Ambient and Liquid Phase Species as a Function of Time for a 4-Hour Rain Event. The data are from a simulation of (and may apply only to) the idealized rain system model shown in Figure 2. No conversion of S(IV) to SO_4^{2-} is assumed to occur in the collector. Conditions: Best raindrop distribution; fall distance = 1000 m; rain rate = 10 mm/hr.; initial rain water pH = 5.63; $[SO_{2(g)}]$ = 20.0 ppb; $[NH_{3(g)}]$ = $[HNO_{3(g)}]$ = 2 ppb; $[O_{3(g)}]$ = 50 ppb; and $[H_2O_{2(g)}]$ = 5 ppb.

22. $[SO_{2(g)}]$ = 40.0 ppb: Concentration of Various Ambient and Liquid Phase Species as a Function of Time for a 4-Hour Rain Event. The data are from a simulation of (and may apply only to) the idealized rain system model shown in Figure 2. No conversion of S(IV) to SO_4^{2-} is assumed to occur in the collector. Conditions: Best raindrop distribution; fall distance = 1000 m; rain rate = 10 mm/hr.; initial rain water pH = 5.63; $[SO_{2(g)}]$ = 40.0 ppb; $[NH_{3(g)}]$ = $[HNO_{3(g)}]$ = 2 ppb; $[O_{3(g)}]$ = 50 ppb; and $[H_2O_{2(g)}]$ = 5 ppb.

REFERENCES

1. Oden, S. The Acidification of Air and Precipitation and its Consequencies on the Natural Environment (Swedish Nat. Sci. Res. Council, Ecology Committee, Bul. 1, 1968).

2. Oden, S. The Acidity Problem--An Outline of Concepts. In: Proceedings of the First International Symposium on Acid Precipitation and the Forest Ecology, May 12-15, 1975, Columbus, OH (USDA Forest Service General Technical Report NE-23, 1976), pp.1-30.

3. Acid Precipitation Act, Title VII of the Energy Security Act of 1980, Public Law 96-294, The Congress of The United States of America (1980).

4. National Acid Precipitation Assessment Plan--June 1982, Interagency Task Force on Acid Precipitation (Executive Director, 722 Jackson Place, NW, Washington, D.C., 1982).

5. Baboolal, L.B., H.R. Pruppacher, and J.H. Topalian. "A Sensitivity Study of a Theoretical Model of SO_2 Scavenging by Water Drops in Air." J. Atmos. Sci., 38:856-870 (1981).

6. Frossling, N. "The Evaporation of Falling Drops." Gerlands Beits. Geophys., 52:170-216 (1938).

7. Markowitz, A.H. "Raindrop Size Distribution Expressions." J. Appl. Met., 15:1029-1031 (1976).

8. Best, A.C. "The Size Distribution of Raindrops." Quart. J. Roy. Met. Soc., 76:16-36 (1950).

9. Perry, R.H. and C.H. Chilton, Ed. Chemical Engineer's Handbook, 5th ed. (McGraw-Hill Book Company, 1973).

10. Hales, J.M. and S.L. Sutter. "Solubility of Sulfur Dioxide in Water at Low Concentrations." Atmos. Environ., 1:997-1001 (1973).

11. Abel, E. and E. Neusser. Uber den Dampfdruck der Salptrigen Saure." Monatshafte fuer Chemie, 54:855-873 (1929).

12. McKay, H.A.C. "The Activity Coefficient of Nitric Acid, A Partially Ionized 1:1-Electrolyte." Transactions of the Faraday Society, 52:1568-1573 (1956).

13. Martin, L.R. and D.E. Damschen. "Aqueous Oxidation of Sulfur Dioxide by Hydrogen Peroxide at Low pH." Atmos. Environ., 15:1615-1621 (1981).

14. Fish, B.R. and J.L. Durham. "Diffusion Coefficient of SO_2 in air." Environ. Letters, 2:13-21 (1971).

15. Gunn, R. and G.D. Kinzer. "The Terminal Velocity of Fall for Water Droplets in Stagnant Air." J. Meteorology, 6:243-248 (1949).

16. Beard, K.V. and H.R. Pruppacher. "A Wind Tunnel Investigation of the Rate of Evaporation of Small Water Drops Falling at Terminal Velocity in Air." J. Atmos. Sci., 28:1455-1464 (1971).

17. Carmichael, G.R. and L.K. Peters. "Some Aspects of SO_2 Absorption by Water--Generalized Treatment." Atmos. Environ., 13:1505-1513 (1979).

18. Marshall, J.S. and W. McK. Palmer. "The Distribution of Raindrops with Size." J. Meteor., 5:165-166 (1948).

19. Levine, S.Z. and S.E. Schwartz. "In-Cloud and Below-Cloud Scavenging of Nitric Acid Vapor." Atmos. Environ., 16:1725-1735 (1982).

20. Eigen, M., W. Kruse, G. Maass, and L. DeMaeyer. "Rate Constants of Protolytic Reactions in Aqueous Solution." Progress in Reaction Kinetics, Volume 2 (G. Porter, ed., MacMillan, NY, 1964), pp.287-318.

21. Himmelblau, D.M. and A.L. Babb. "Reaction Rate Constants by Radioactive Tracer Techniques." Industrial and Engineering Chemistry, 51:1403-1408 (1959).

22. Ericson, R.E. and L.M. Yates. "Reaction Kinetics of Ozone with Sulfur Compounds." U.S. Environmental Protection Agency. EPA-600/3-76-089 (1976), 69pp.

23. Ericson,R.E., L.M. Yates, R.L. Clard, and C.M. McEwen. "The Reaction of Sulfur Dioxide with Ozone in Water and its Possible Atmospheric Significance." Atmos. Environ., 11:813-817 (1977).

24. Dasgupta, P.K. Letter in: Atmos. Environ., 14:227-275 (1980).

25. Hoffman, M.R. and J.O. Edwards. "Kinetics of the Oxidation of Sulfite by Hydrogen Peroxide in Acidic Solution." J. Phys. Chem., 79:2096-2098 (1975).

26. Penkett, S.A., M.R. Jones, K.A. Brice, and A.E.J. Eggleton. "The Importance of Atmospheric Ozone and Hydrogen Peroxide in Oxidizing Sulfur Dioxide in Cloud and Rain Water." Atmos. Environ., 13:123-137 (1979).

27. Penkett, S.A., M.R. Jones, and A.E.J. Eggleton. "A Study of SO_2 Oxidation in Stored Rainwater Samples." Atmos. Environ., 13:139-147 (1979).

28. Brodzinsky, R., S.G. Chang, S.S. Markowitz, and T. Novakov. "Kinetics and Mechanism for the Catalytic Oxidation of Sulfur Dioxide on Carbon in Aqueous Suspensions." J. Phys. Chem., 84:3354-3358 (1980).

29. Penkett, S.A. "Oxidation of SO_2 and Other Atmospheric Gases by Ozone in Aqueous Solution." Nature, 240:105-106 (1972).

30. Overton, J.H., Jr., V.P. Aneja, and J.L. Durham. "Production of Sulfate in Rain and Raindrops in Polluted Atmospheres." Atmos. Envron., 13:355-367 (1979).

31. Brimblecombe, P. and D.J. Spedding. "The Catalytic Oxidation of Micromolar Aqueous Sulfur Dioxide. I. Oxidation in Solutions Containing Iron(III)." Atmos. Environ., 8:937-945 (1974).

32. Durham, J.L., J.H. Overton, Jr., V.P. Aneja. "Influence of Gaseous Nitric Acid on Sulfate Production and Acidity in Rain." Atmos. Environ., 15:1059-1068 (1981).

33. Gertler, A.W., D.F. Miller, D. Lamb, and U. Katz. "Studies of SO_2 and NO_2 Reactions in Haze and Clouds." (This Volume.)

34. Martin, L.R., D.E. Damschen, and H.S. Judeikis. "Sulfur Dioxide Oxidation Reactions in Aqueous Solutions." U.S. Environmental Protection Agency, EPA-600/S7-81-085 (1981).

35. Gay, B.W. and J.J. Bufalini. "Hydrogen Peroxide in the Urban Atmosphere." In: Photochemical Smog and Ozone Reactions, ACS Advances in Chemistry Series, Vol. 113, pp.255-263 (1972).

36. Spicer, C.W. "Measurement of Gaseous HNO_3 by Electrochemistry and Chemiluminescence." In: Current Methods to Measure Atmospheric Nitric Acid and Nitric Acid Artifacts, U.S. Environmental Protection Agency, EPA-600/2-79-051, pp.27-35 (1979).